

# Statistical Mechanics of Support Vector Regression

Abdulkadir Canatar and SueYeon Chung

Center for Computational Neuroscience, Flatiron Institute, New York, NY, 10010

Center for Neural Science New York University, New York, NY, 10003, USA

(Dated: December 10, 2024)

A key problem in deep learning and computational neuroscience is relating the geometrical properties of neural representations to task performance. Here, we consider this problem for continuous decoding tasks where neural variability may affect task precision. Using methods from statistical mechanics, we study the average-case learning curves for  $\varepsilon$ -insensitive Support Vector Regression ( $\varepsilon$ -SVR) and discuss its capacity as a measure of linear decodability. Our analysis reveals a phase transition in the training error at a critical load, capturing the interplay between the tolerance parameter  $\varepsilon$  and neural variability. We uncover a double-descent phenomenon in the generalization error, showing that  $\varepsilon$  acts as a regularizer, both suppressing and shifting these peaks. Theoretical predictions are validated both on toy models and deep neural networks, extending the theory of Support Vector Machines to continuous tasks with inherent neural variability.

*Introduction.*— Modern machine learning applications often require the ability to perform tasks that remain invariant under certain transformations of input data. For instance, decoding of a class should remain unaffected by variations in the object’s representations due to factors like translations [1]. Deep neural networks achieve this by learning a meaningful representation of input data, from which decoding the information relevant to the task becomes easier. For instance, an effective representation’s decoding should be invariant to task-irrelevant transformations while remaining covariant with respect to task-relevant information. Understanding such geometric properties of neural representations is essential for unraveling the computational mechanisms implemented by neural networks [2–4].

Previous studies have explored the geometrical properties of neural representations in relation to invariant prediction, particularly focusing on the linear decodability under neural variability [4–6]. However, these studies largely concentrate on classification tasks, despite the fact that decoding continuous variables, such as an object’s position or orientation, is essential in fields like control and robotics where precise and continuous outputs are critical. This leaves a gap in our understanding of how effective decoding of continuous variables can be achieved in the presence of neural variability.

In this letter, we study  $\varepsilon$ -insensitive Support Vector Regression ( $\varepsilon$ -SVR) algorithm [7, 8] to analyze continuous tasks with input data variances. The  $\varepsilon$ -SVR task is similar to the ridge regression, except that the objective is satisfied when the prediction error lies within a tube of size  $\varepsilon$  (Fig. 1). Here, the *tube size*  $\varepsilon$  is a hyperparameter that defines the margin of tolerance for input deviations and needs to be fine-tuned. Using the replica method [9–11], we develop an analytical theory of generalization in  $\varepsilon$ -SVR that relates the geometry of invariances to the precision of decoding a continuous variable. Our theory recovers the previous results on ridge regression in the limit  $\varepsilon \rightarrow 0$  [12–18].

*Theoretical Framework.*— We assume a supervised learning setup where the input data is represented by  $N$ -dimensional *center* representations  $\bar{\psi}$ , and the labels  $\bar{y}$  are linearly generated by a coding direction  $\bar{\mathbf{w}}$ , i.e.  $\bar{y} = \bar{\mathbf{w}} \cdot \bar{\psi}$ . Here, centers  $\bar{\psi}$  are treated as random variables and capture the task-relevant information from the input data.

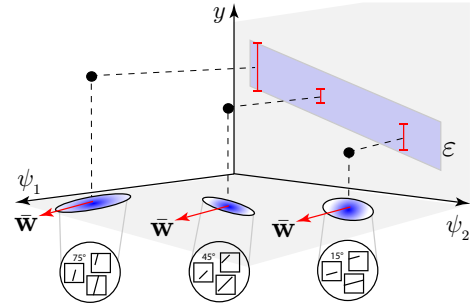


FIG. 1. Decoding the angle of sticks from their images as an example of invariant regression. Blue regions depict the encoding representations in  $(\psi_1, \psi_2)$ -space induced by nuisance variances for each angle with varying geometries. They depict possible noise geometries with  $\delta$  parallel (left), orthogonal (middle), and partially aligned (right) with the coding direction  $\bar{\mathbf{w}}$ .

In contrast, the algorithm receives *encoding* representations  $\psi$  which include both the task-relevant centers  $\bar{\psi}$  and task-irrelevant variations modeled by random variables  $\delta$ , and assumed to be of the form  $\psi \equiv \bar{\psi} + \delta$ . The *noise* representations  $\delta$  represent nuisance variations around the centers. The goal is to learn a linear predictor  $y = \mathbf{w} \cdot \psi$ .

At each instantiation of a training set,  $P$ -samples  $\{\bar{\psi}^\mu, \psi^\mu\}_{\mu=1}^P$  are drawn i.i.d. from their respective distributions, and labels  $\bar{y}^\mu$  and predictions  $y^\mu$  are generated. Due to the additional noise, the predictions always mismatch with the labels when  $P > N$  and overfit to noise when  $P < N$ . To account for this variance, we consider

the  $\varepsilon$ -SVR algorithm

$$\min_{\mathbf{w} \in \mathbb{R}^N} \frac{1}{2} \|\mathbf{w}\|^2 + \frac{1}{2\lambda} \sum_{\mu=1}^P [|y^\mu - \bar{y}^\mu| - \varepsilon]_+^2 \quad (1)$$

where  $\varepsilon$  is the tube size,  $\lambda$  is the ridge parameter and  $[x]_+ \equiv \max(0, x)$ . We note that both  $\lambda$  and  $\varepsilon$  act as a regularizer for regression since both control the effect of training error in the final solution. However, we found that they qualitatively have different effects on generalization (see SI.A). While our calculation is valid for arbitrary  $\lambda$  and  $\varepsilon$ , for our purposes we only consider the ridgeless case ( $\lambda = 0$ ) which enforces vanishing training error.

Our goal is to compute the average-case training and generalization errors for  $\varepsilon$ -SVR. By treating the training set as a quenched disorder, we compute these average quantities using the replica method of statistical physics and consider the following partition function

$$\overline{\log Z} = \overline{\log \int d\mathbf{w} e^{-NS(\mathbf{w}, \boldsymbol{\psi}^\mu, \bar{\boldsymbol{\psi}}^\mu) + J\mathcal{O}(\mathbf{w})}} \quad (2)$$

$$S = \frac{1}{2N} \|\mathbf{w}\|^2 + \frac{1}{2\lambda N} \sum_{\mu=1}^P \left[ |\mathbf{w} \cdot \boldsymbol{\psi}^\mu - \bar{\mathbf{w}} \cdot \bar{\boldsymbol{\psi}}^\mu| - \varepsilon \right]_+^2,$$

where the overline denotes the quenched average over the training set  $\{\boldsymbol{\psi}^\mu, \bar{\boldsymbol{\psi}}^\mu\}$  of size  $P$ . In the thermodynamic limit  $P, N \rightarrow \infty$  while keeping  $\alpha \equiv P/N \sim \mathcal{O}(1)$ , the free energy  $S$  in Eq. 2 becomes self-averaging and concentrates around the solution to the problem in Eq. 1. Then, the average of any observable  $\langle \mathcal{O}(\mathbf{w}) \rangle$  can be computed by taking derivatives of  $\overline{\log Z}$  with respect to source  $J$ . The training error  $E_{tr}$  and generalization error  $E_g$ , the two observables we are interested in, are given by

$$E_{tr} = \overline{\frac{1}{P} \sum_{\mu=1}^P \left[ |\mathbf{w} \cdot \boldsymbol{\psi}^\mu - \bar{\mathbf{w}} \cdot \bar{\boldsymbol{\psi}}^\mu| - \varepsilon \right]_+^2}$$

$$E_g = \overline{\left\langle (\mathbf{w} \cdot \boldsymbol{\psi} - \bar{\mathbf{w}} \cdot \bar{\boldsymbol{\psi}})^2 \right\rangle_{\boldsymbol{\psi}, \bar{\boldsymbol{\psi}}}}. \quad (3)$$

*Replica Calculation.*— For simplicity, we consider a joint Gaussian distribution of center and encoding representations as

$$\begin{bmatrix} \boldsymbol{\psi} \\ \bar{\boldsymbol{\psi}} \end{bmatrix} \sim \mathcal{N} \left( 0, \begin{bmatrix} \boldsymbol{\Sigma}_{\boldsymbol{\psi}} & \boldsymbol{\Sigma}_{\boldsymbol{\psi}\bar{\boldsymbol{\psi}}} \\ \boldsymbol{\Sigma}_{\boldsymbol{\psi}\bar{\boldsymbol{\psi}}}^\top & \boldsymbol{\Sigma}_{\bar{\boldsymbol{\psi}}} \end{bmatrix} \right). \quad (4)$$

Note that the solution to the objective in Eq. 2 under this data distribution depends highly on the correlation between centers  $\bar{\boldsymbol{\psi}}$  and encoding representations  $\boldsymbol{\psi}$ . Specifically, in the limit  $P \rightarrow \infty$ , optimal weights and the generalization error asymptotes to:

$$E_\infty = \text{tr } \bar{\mathbf{w}} \bar{\mathbf{w}}^\top \boldsymbol{\Sigma}_{\bar{\boldsymbol{\psi}}} - \text{tr } \mathbf{w}_* \mathbf{w}_*^\top \boldsymbol{\Sigma}_{\boldsymbol{\psi}}, \quad \mathbf{w}_* = \boldsymbol{\Sigma}_{\boldsymbol{\psi}}^{-1} \boldsymbol{\Sigma}_{\boldsymbol{\psi}\bar{\boldsymbol{\psi}}} \bar{\mathbf{w}},$$

where  $\text{tr}$  denotes the normalized trace operator,  $\mathbf{w}_*$  is the target weights projected to the learnable subspace, and

$E_\infty$  is the irreducible error corresponding to the unexplainable variance in the target [17].

Performing the quenched average with this distribution under the replica symmetric ansatz and a saddle point approximation (see SI.A for details), the mean-field solution is described by three effective quantities: the *effective regularization*  $\tilde{\lambda}$ , *effective tube size*  $\tilde{\varepsilon}$  and the *effective load*  $\tilde{\alpha}$ :

$$\tilde{\lambda} = \lambda + \mathcal{F}(\tilde{\lambda}, \tilde{\varepsilon}), \quad \tilde{\varepsilon} = \varepsilon / \sqrt{\mathcal{G}(\tilde{\lambda}, \tilde{\varepsilon})}, \quad \tilde{\alpha} = \alpha f(\tilde{\varepsilon}) \quad (5)$$

where  $\tilde{\lambda}$  and  $\tilde{\varepsilon}$  obey the coupled self-consistent equations

$$\mathcal{F}(\tilde{\lambda}, \tilde{\varepsilon}) = \text{tr } \boldsymbol{\Sigma}_{\boldsymbol{\psi}} \mathbf{G}^{-1}, \quad \mathbf{G} = \mathbf{I} + \frac{\tilde{\alpha}}{\tilde{\lambda}} \boldsymbol{\Sigma}_{\boldsymbol{\psi}}, \quad \gamma = \partial_{\tilde{\lambda}} \mathcal{F}(\tilde{\lambda}, \tilde{\varepsilon})$$

$$\mathcal{G}(\tilde{\lambda}, \tilde{\varepsilon}) = \frac{E_\infty + \text{tr } \mathbf{w}_* \mathbf{w}_*^\top \boldsymbol{\Sigma}_{\boldsymbol{\psi}} \mathbf{G}^{-2}}{1 - g(\tilde{\varepsilon}) \gamma} \quad (6)$$

where the functions  $f(\tilde{\varepsilon})$  and  $g(\tilde{\varepsilon})$  are defined as

$$f(\tilde{\varepsilon}) = \left\langle \theta(|z| - \tilde{\varepsilon}) \right\rangle_z, \quad g(\tilde{\varepsilon}) = \frac{\left\langle (|z| - \tilde{\varepsilon})^2 \theta(|z| - \tilde{\varepsilon}) \right\rangle_z}{\left\langle \theta(|z| - \tilde{\varepsilon}) \right\rangle_z}$$

where  $\langle f(z) \rangle_z$  denotes integration over  $z$  with respect to standard normal distribution. Furthermore, the function  $\mathcal{G}(\tilde{\lambda}, \tilde{\varepsilon})$  coincides with the generalization error defined in Eq. 3.

Effective regularization  $\tilde{\lambda}$  is the renormalized ridge parameter [18, 19] that controls the smoothness of the solution and quantifies the implicit regularization of the model [13, 14].

Effective load  $\tilde{\alpha}$  gives a measure of the actual number of samples that contribute to learning, and decreases monotonically as a function of effective tube size  $\tilde{\varepsilon}$ . Intuitively, larger tube sizes require sampling more points since it becomes less likely to hit the tube boundary. A similar definition had been also derived in [20] when the learning is restricted to a subset of training examples.

Effective tube size  $\tilde{\varepsilon}$ , on the other hand, is the renormalized tube size and depends inversely on the generalization error, implying that the number of samples required to improve generalization increases as the model's predictivity improves (Eq. 5). Finally,  $\tilde{\varepsilon}$  can also be considered as effective discriminability as a function of  $\alpha$ , where *discriminability*  $d' \equiv \varepsilon / \sqrt{E_\infty}$  is a common metric used in neuroscience [21, 22], quantifying the perceptible contrast between two stimuli  $\varepsilon$ -apart from each other.

*Analysis of a Toy Data Model.*— To analyze our results and build intuition, we apply our theory to investigate the decoding precision in the presence of structured noise, which correlates with the coding direction. We consider a toy data model where the centers are drawn from  $\bar{\boldsymbol{\psi}} \sim \mathcal{N}(0, \mathbf{I})$  and the labels are generated by  $\bar{y} = \bar{\mathbf{w}} \cdot \bar{\boldsymbol{\psi}}$  with  $\text{tr } \bar{\mathbf{w}} \bar{\mathbf{w}}^\top = 1$ . The representations seen by the linear model are of the form  $\boldsymbol{\psi} = \bar{\boldsymbol{\psi}} + \sigma \boldsymbol{\delta}$  where the noise  $\boldsymbol{\delta}$  is drawn

from a structured Gaussian distribution with zero mean and covariance

$$\Sigma_\delta = (1 - \beta)\mathbf{P} + \beta(\mathbf{I} - \mathbf{P}), \quad \mathbf{P} \equiv \mathbf{I} - \frac{1}{N}\bar{\mathbf{w}}\bar{\mathbf{w}}^\top, \quad (7)$$

and  $\sigma$  controls the strength of noise. Through the parameter  $\beta$ , this noise model interpolates between the cases where the noise is completely orthogonal ( $\beta = 0$ ) or parallel ( $\beta = 1$ ) to the coding direction  $\bar{\mathbf{w}}$ . A schematic of this data model is depicted in Fig. 1.

For this model, the resulting training and generalization errors in Eq. 3 (SI.C) read

$$E_g = \frac{1}{1 - \frac{g(\tilde{\varepsilon})\tilde{\alpha}}{(\tilde{\alpha} + \tilde{\lambda})^2}} \left( E_\infty + \frac{1 - E_\infty}{\left(1 + \frac{\tilde{\alpha}}{\tilde{\lambda}} \frac{1 + \beta\sigma^2}{1 + (1 - \beta)\sigma^2}\right)^2} \right)$$

$$E_{tr} = \left(1 - \frac{1}{\tilde{\alpha} + \tilde{\lambda}}\right)^2 f(\tilde{\varepsilon})g(\tilde{\varepsilon})E_g, \quad E_\infty = \frac{\beta\sigma^2}{1 + \beta\sigma^2}, \quad (8)$$

where the self-consistent equations for  $\tilde{\lambda}$  and  $\tilde{\varepsilon}$  in Eq. 5 can be solved numerically. Furthermore, in the ridgeless limit  $\lambda \rightarrow 0$ , the equation for  $\tilde{\lambda}$  simplifies to

$$\tilde{\lambda} = \begin{cases} 1 - \tilde{\alpha}, & \tilde{\alpha} < 1 \\ 0, & \tilde{\alpha} \geq 1. \end{cases} \quad (9)$$

This implies that in the over-parameterized regime, when the effective sample size is smaller than the number of parameters, the training error vanishes identically and goes through a first-order phase transition at  $\tilde{\alpha} = 1$ , beyond which it becomes proportional to  $E_g$ . Additionally, the generalization error in Eq. 8 becomes proportional to  $E_\infty$  when  $\tilde{\alpha} > 1$ , implying that it also vanishes whenever  $\beta$  or  $\sigma$  vanishes. In Fig. 2, we plot the free energy for various model parameters demonstrating the phase transition. In

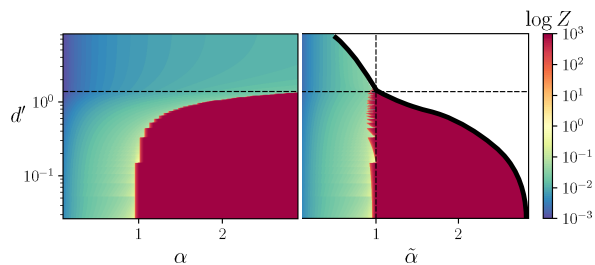


FIG. 2. Phase plots of the theoretical values of  $\overline{\log Z}$  against  $d' = \varepsilon/\sqrt{E_\infty}$ . (Left) For fixed  $E_\infty$ , increasing  $\varepsilon$  delays phase transition, and for fixed  $\varepsilon$ , increasing noise variability ( $\sigma$ ) causes a phase transition for smaller sample sizes. (Right) Same plot but as a function of  $\tilde{\alpha}$ . Vertical dashed line indicates the phase boundary at  $\tilde{\alpha} = 1$ , and horizontal lines separate the cases below and above the capacity.

the limit  $\varepsilon \rightarrow 0$ , our theory recovers the equations from previous work on ridge regression [13, 14, 23]. However,

we discover additional phenomena in SVR that lack in ridge regression and are reported below.

*Model Capacity and Effective Sample Size.*— Our results show that the phase boundary is described by the effective load  $\tilde{\alpha} = 1$  (see Fig. 2). This is demonstrated both for  $E_{tr}$  and  $E_g$  in Fig. 3, where we also observe an excellent agreement with experiments.

For training error  $E_{tr}$ , the phase transition happens at  $\alpha = 1$  in ridge regression ( $\varepsilon = 0$ ), while in SVR ( $\varepsilon > 0$ ) the transition occurs for larger  $\alpha > 1$  (Fig. 3a). This is expected since larger tube sizes allow for more *capacity* in the sense that more samples can be fit satisfying  $E_{tr} = 0$ . Hence, the transition for non-zero  $\varepsilon$  occurs at some critical load  $\alpha_c > 1$

$$\alpha_c^{-1} = f(\tilde{\varepsilon}) \quad (10)$$

which satisfies  $\tilde{\alpha} = 1$  (see Fig. 3a inset). The critical load  $\alpha_c$  is the maximum amount of training examples that can be fit within an  $\varepsilon$ -tube and, in analogy to classification capacity [5], can be used as a measure that ties representational geometry to the precision of continuous decoding tasks.

The computation of  $\alpha_c$  requires solving the equations in Eq. 5 which are in general analytically intractable. However, it can be exactly solved for our toy model Eq. 8 at the criticality (see SI.C). The solution asymptotically behaves as

$$\tilde{\varepsilon} \approx \begin{cases} d' - 1/d', & d' \gg 1 \\ d'^2 \sqrt{\frac{2}{\pi}}, & d' \ll 1 \end{cases}, \quad (11)$$

which gives an explicit relation between  $\alpha_c$  and the perceptual discriminability through Eq. 10, and captures the fact that imposing lower discriminability allows fitting more samples with zero training error. Furthermore, it

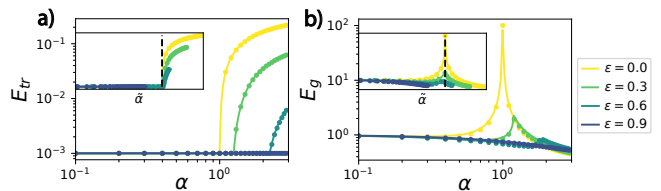


FIG. 3. Theoretical (lines) and experimental (dots) learning curves for the toy model with  $\beta = 0.5$  and  $\sigma = 1$ . Insets show the same curves but as a function of  $\tilde{\alpha}$ . **a)** With increasing  $\varepsilon$ -tube size, training error decreases due to increasingly relaxed definition of being correct, therefore allowing more samples to be fit. **b)** On the other hand, generalization error displays a non-monotonicity called the double-descent. In this case, the effect of increasing  $\varepsilon$  amounts to keeping the problem in the *overparameterized* regime.

allows us to connect the representational properties to the capacity since  $d'$  depends on  $\sigma$  and  $\beta$ . For fixed tube size  $\varepsilon$ , discriminability  $d'$  increases with more noise and task

correlation. On the other hand, when the noise geometry is completely orthogonal to the task ( $\beta = 0$ ), the noise magnitude does not affect  $d'$  and hence the capacity.

*Double-Descent and Optimal Learning Rates.*— The analysis of  $E_g$  reveals a well-known phenomenon known as *double-descent* [24, 25] where the generalization worsens with more data near the critical point  $\tilde{\alpha} = 1$  (see Fig. 3b). Essentially, double-descent implies overfitting to noisy samples at the model capacity and is indicative of a transition between over and under-parameterized regimes.

In ridge regression, this overfitting can be avoided by tuning the ridge parameter  $\lambda$  that penalizes solutions with large norms [26]. In our case, despite we set ridge regularization to zero, turning on  $\varepsilon$  also acts like a regularization. However, in contrast to the ridge penalty, which only suppresses the double-descent peak,  $\varepsilon$  also shifts the peak, implying that the tube size effectively controls whether the model is in over or under-parameterized regime (Fig. 3b).

Our theory allows us to compute the optimal learning rates by finding the parameters  $\lambda$  and  $\varepsilon$  that minimize  $E_g$ . Here, we compute optimal  $\varepsilon$  for SVR and optimal  $\lambda$  for ridge regression which was also studied previously in [27–30] (see SI.B).

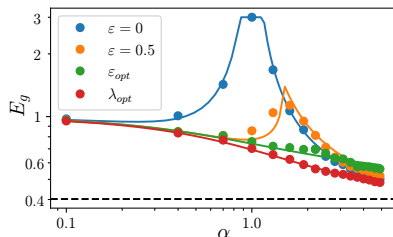


FIG. 4. Optimal learning curves for the toy model. Choosing optimal  $\lambda$  always outperforms optimal  $\varepsilon$ . Lines indicate theory, and dots indicate experiments. The dashed line indicates  $E_{\infty}$ .

Optimal ridge regression leads to non-zero training error, while optimal SVR ensures zero training error for all  $\alpha$ . We find that the former always outperforms the latter (see Fig. 4). This is because optimal SVR stops sending error signals as soon as the constraints are satisfied, while in ridge regression, the model is forced to learn finer details since the training error never vanishes.

*Real Data Applications.*— Although our theory is valid in the self-averaging limit  $N \rightarrow \infty$  and  $\alpha \sim \mathcal{O}(1)$ , we find that it agrees well with experiments when it is applied to real data with finite  $P$  and  $N$  (see SI.E).

To illustrate our theory’s applicability to real data, we develop an experiment where the task is to estimate the orientation of grating images from their deep neural network representations. We generate grating images with orientations  $\theta$  drawn uniformly from  $[0, \pi)$ , and augment each image with task-irrelevant attributes such as the frequency and phase of gratings (see SI.E). We obtain their neural network representations from the hidden layers of a class of ResNet architectures and evaluate them by

computing their decoding performance based on optimal  $\varepsilon$ -SVR.

In Fig. 5, we show the optimal  $\varepsilon_{opt}$  and generalization error for both randomly initialized models and trained models on natural scenes. Here,  $\varepsilon_{opt}$  is normalized by the range of the decoding interval  $L$  such that the case  $\varepsilon_{opt}/L > 1$  implies that decoding any orientation is impossible while fitting all training examples. For random networks, we find that discriminability improves for deeper layers, while for trained networks, middle layers perform better and discriminability gets worse in deeper layers. The observation that early layers of deep networks perform better for simple stimuli like gratings was previously made in [31].

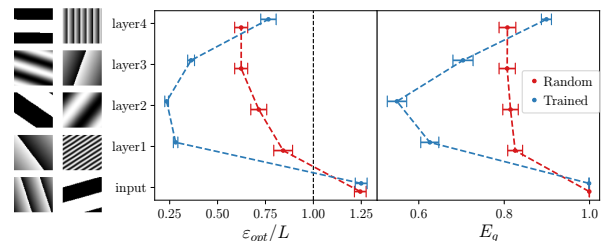


FIG. 5. SVR analysis of layers extracted from trained and random ResNet models on the task of decoding grating orientations.

Our theory enables the decomposing of generalization error into various spectral properties of the data, providing further insights into why generalization error evolves across the network layers. In SI.D, we show that the error mode geometry analysis introduced in [32] can be directly applied to our theory (see SI.F 2 for error mode geometry analysis).

*Discussion.*— Invariant decoding remains a critical challenge in machine learning and neuroscience, as real-world inputs frequently vary in ways that do not alter the target attribute. This study bridges the gap between representational geometry and its influence on continuous decoding tasks. By utilizing  $\varepsilon$ -SVR as a geometric probe in high-dimensional feature spaces, we employed average-case analysis to explore how the geometry of noise representations impacts decoding performance.

In particular, our analysis revealed that the phase transition in the training error can be controlled by the tube size parameter  $\varepsilon$  which also sets the target precision of the task. Larger  $\varepsilon$  values increase the model’s capacity by allowing more samples to be fit without error, but this comes at the cost of reduced precision in continuous variable decoding, as indicated by increased generalization error. The balance between training error and generalization error underscores the importance of tuning  $\varepsilon$  to optimize both model fit and predictive accuracy.

While our analysis currently relies on Gaussian assumptions and linear decoding strategies, future investigations should extend beyond these assumptions, addressing more



realistic scenarios of coding in distributed neural representations.

Our theoretical framework reveals fundamental trade-offs between precision and robustness in neural computations. The relationship we uncovered between representational geometry and decoding performance not only enhances our understanding of SVR algorithms but could also inform the design of more robust regression models and understand the nature of neural decoding algorithms where precise representations must be maintained despite inherent variability.

- 
- [1] Y. LeCun, Y. Bengio, and G. Hinton, *nature* **521**, 436 (2015).
- [2] Y. Bengio, A. Courville, and P. Vincent, *IEEE transactions on pattern analysis and machine intelligence* **35**, 1798 (2013).
- [3] A. Achille and S. Soatto, *Journal of Machine Learning Research* **19**, 1 (2018).
- [4] S. Chung and L. Abbott, *Curr. opin. neurobiol.* **70**, 137 (2021).
- [5] S. Chung, D. D. Lee, and H. Sompolinsky, *Physical Review X* **8**, 031003 (2018).
- [6] A. J. Wakhloo, T. J. Sussman, and S. Chung, *Physical Review Letters* **131**, 027301 (2023).
- [7] H. Drucker, C. J. C. Burges, L. Kaufman, A. Smola, and V. Vapnik, in *Advances in Neural Information Processing Systems*, Vol. 9, edited by M. Mozer, M. Jordan, and T. Petsche (MIT Press, 1996).
- [8] B. Schölkopf, A. J. Smola, R. C. Williamson, and P. L. Bartlett, *Neural computation* **12**, 1207 (2000).
- [9] M. Mézard, G. Parisi, and M. A. Virasoro, *Spin glass theory and beyond: An Introduction to the Replica Method and Its Applications*, Vol. 9 (World Scientific Publishing Company, 1987).
- [10] A. Engel, *Statistical mechanics of learning* (Cambridge University Press, 2001).
- [11] M. Mezard and A. Montanari, *Information, physics, and computation* (Oxford University Press, 2009).
- [12] B. Bordelon, A. Canatar, and C. Pehlevan, in *International Conference on Machine Learning* (PMLR, 2020) pp. 1024–1034.
- [13] A. Jacot, B. Simsek, F. Spadaro, C. Hongler, and F. Gabriel, in *International Conference on Machine Learning* (PMLR, 2020) pp. 4631–4640.
- [14] A. Canatar, B. Bordelon, and C. Pehlevan, *Nature communications* **12**, 2914 (2021).
- [15] B. Loureiro, C. Gerbelot, H. Cui, S. Goldt, F. Krzakala, M. Mezard, and L. Zdeborová, *Advances in Neural Information Processing Systems* **34**, 18137 (2021).
- [16] J. B. Simon, M. Dickens, D. Karkada, and M. Dewese, *Transactions on Machine Learning Research* (2023).
- [17] A. Atanasov, B. Bordelon, S. Sainathan, and C. Pehlevan, in *The Eleventh International Conference on Learning Representations* (2022).
- [18] A. B. Atanasov, J. A. Zavatone-Veth, and C. Pehlevan, *Scaling and renormalization in high-dimensional regression* (2024), [arXiv:2405.00592](https://arxiv.org/abs/2405.00592) [[stat.ML](https://arxiv.org/html/2405.00592v1)].
- [19] C. Cheng and A. Montanari, *Dimension free ridge regression* (2022), [arXiv:2210.08571](https://arxiv.org/abs/2210.08571) [[math.ST](https://arxiv.org/html/2210.08571v1)].
- [20] S. Bös, W. Kinzel, and M. Opper, *Physical Review E* **47**, 1384 (1993).
- [21] H. S. Seung and H. Sompolinsky, *Proceedings of the national academy of sciences* **90**, 10749 (1993).
- [22] N. Brunel and J.-P. Nadal, *Neural computation* **10**, 1731 (1998).
- [23] B. Adlam and J. Pennington, in *International Conference on Machine Learning* (PMLR, 2020) pp. 74–84.
- [24] M. Belkin, S. Ma, and S. Mandal, in *International Conference on Machine Learning* (PMLR, 2018) pp. 541–549.
- [25] M. Belkin, D. Hsu, S. Ma, and S. Mandal, *Proceedings of the National Academy of Sciences* **116**, 15849 (2019).
- [26] B. Schölkopf, A. J. Smola, F. Bach, *et al.*, *Learning with kernels: support vector machines, regularization, optimization, and beyond* (MIT press, 2002).
- [27] C. Thrampoulidis, S. Oymak, and B. Hassibi, in *Conference on Learning Theory* (PMLR, 2015) pp. 1683–1709.
- [28] D. Wu and J. Xu, *Advances in Neural Information Processing Systems* **33**, 10112 (2020).
- [29] D. Kobak, J. Lomond, and B. Sanchez, *The Journal of Machine Learning Research* **21**, 6863 (2020).
- [30] Z. Zhang, *arXiv preprint arXiv:2405.19398* (2024).
- [31] H. Hong, D. L. Yamins, N. J. Majaj, and J. J. DiCarlo, *Nature neuroscience* **19**, 613 (2016).
- [32] A. Canatar, J. Feather, A. Wakhloo, and S. Chung, *Advances in Neural Information Processing Systems* **36** (2024).
- [33] S. Mei, T. Misiakiewicz, and A. Montanari, *Applied and Computational Harmonic Analysis* **59**, 3 (2022).
- [34] S. Mei and A. Montanari, *Communications on Pure and Applied Mathematics* **75**, 667 (2022).
- [35] H. Hu and Y. M. Lu, *arXiv preprint arXiv:2205.06798* (2022).
- [36] T. Misiakiewicz and B. Saeed, *A non-asymptotic theory of kernel ridge regression: deterministic equivalents, test error, and gcv estimator* (2024), [arXiv:2403.08938](https://arxiv.org/abs/2403.08938) [[stat.ML](https://arxiv.org/html/2403.08938v1)].
- [37] A. Maloney, D. A. Roberts, and J. Sully, *arXiv preprint arXiv:2210.16859* (2022).

## Appendix A: Problem Setup

Here, we study a family of regression problems and their generalization properties using the replica method. In our notation, we consider a training set  $\mathcal{D} = \{(\mathbf{x}^\mu, \bar{y}^\mu)\}_{\mu=1}^P$  consisting of  $P$  i.i.d. drawn inputs  $\mathbf{x}^\mu$  and labels  $\bar{y}^\mu$ . In this work, we assume that the target labels are related to the inputs via

$$\bar{y}^\mu = \bar{\mathbf{w}} \cdot \bar{\boldsymbol{\psi}}^\mu, \quad \bar{\boldsymbol{\psi}}^\mu \equiv \bar{\boldsymbol{\psi}}(\mathbf{x}^\mu) \in \mathbb{R}^N, \quad \bar{\mathbf{w}} \in \mathbb{R}^N, \quad (\text{A1})$$

where  $\bar{\boldsymbol{\psi}}^\mu$  denote  $N$ -dimensional *center* features as a function of input samples, and  $\bar{\mathbf{w}}$  denotes the *coding direction*. On the other hand, we consider a linear predictor

$$y^\mu = \mathbf{w} \cdot \boldsymbol{\psi}^\mu, \quad \boldsymbol{\psi}^\mu \equiv \boldsymbol{\psi}(\mathbf{x}^\mu) \in \mathbb{R}^N, \quad \mathbf{w} \in \mathbb{R}^N, \quad (\text{A2})$$

where  $\boldsymbol{\psi}^\mu$  denote the  $N$ -dimensional *encoding* features available to the predictor, and  $\mathbf{w}$  is to be learned.

Our generic regression task solves the following problem:

$$\min_{\mathbf{w}} \frac{1}{2} \|\mathbf{w}\|^2 + \frac{1}{\lambda} \sum_{\mu=1}^P \ell(\mathbf{w} \cdot \boldsymbol{\psi}^\mu - \bar{\mathbf{w}} \cdot \bar{\boldsymbol{\psi}}^\mu), \quad (\text{A3})$$

where  $\ell(x)$  is the loss function. Below we list possible choices for  $\ell(x)$ :

- **Kernel Ridge Regression (KRR):** For ridge regression,  $\ell(x) = \frac{1}{2}x^2$  and the optimization problem becomes:

$$\min_{\mathbf{w}} \frac{1}{2} \|\mathbf{w}\|^2 + \frac{1}{2\lambda} \sum_{\mu=1}^P (\mathbf{w} \cdot \boldsymbol{\psi}^\mu - \bar{\mathbf{w}} \cdot \bar{\boldsymbol{\psi}}^\mu)^2. \quad (\text{A4})$$

Here,  $\lambda \rightarrow 0$  limit corresponds to the ridgeless (least-squares) regression, and the case with linear features ( $\boldsymbol{\psi}(\mathbf{x}) = \mathbf{x}$ ) corresponds to linear regression.

- **Support Vector Regression (SVR):** Specifically, we consider  $\varepsilon$ -insensitive SVR where the loss vanishes if the error is less than some positive tolerance variable  $\varepsilon$ . Generically, the loss function is  $\ell(x) = \frac{1}{n!} \max(0, |x| - \varepsilon)^n$ , and the optimization problem becomes:

$$\min_{\mathbf{w}} \frac{1}{2} \|\mathbf{w}\|^2 + \frac{1}{n!\lambda} \sum_{\mu=1}^P \max(0, |\mathbf{w} \cdot \boldsymbol{\psi}^\mu - \bar{\mathbf{w}} \cdot \bar{\boldsymbol{\psi}}^\mu| - \varepsilon)^n, \quad (\text{A5})$$

where  $n \in \mathbb{N}_0$  are non-negative integers. Note that the case where  $n = 2$  and  $\varepsilon = 0$  is identical to KRR above.

A few notes are in order:

- Our calculations require averaging over this inputs  $\mathbf{x}^\mu$ , which is intractable for general feature maps. However, we make a *Gaussian assumption* that the statistics of  $\bar{\boldsymbol{\psi}}(\mathbf{x}^\mu)$  and  $\boldsymbol{\psi}(\mathbf{x}^\mu)$  can be approximated by their second moments:

$$\langle \bar{\boldsymbol{\psi}}(\mathbf{x}) \bar{\boldsymbol{\psi}}(\mathbf{x})^\top \rangle_{\mathbf{x}} = \frac{1}{N} \boldsymbol{\Sigma}_{\bar{\boldsymbol{\psi}}}, \quad \langle \boldsymbol{\psi}(\mathbf{x}) \boldsymbol{\psi}(\mathbf{x})^\top \rangle_{\mathbf{x}} = \frac{1}{N} \boldsymbol{\Sigma}_{\boldsymbol{\psi}}, \quad \langle \boldsymbol{\psi}(\mathbf{x}) \bar{\boldsymbol{\psi}}(\mathbf{x})^\top \rangle_{\mathbf{x}} = \frac{1}{N} \boldsymbol{\Sigma}_{\boldsymbol{\psi} \bar{\boldsymbol{\psi}}} \quad (\text{A6})$$

and the final results will depend only on these quantities. This approximation simplifies our calculations, yields excellent agreement with experiments, and is also justified by the *Gaussian equivalence* theorems in high dimensional statistics where the covariance of non-linear features (kernels) can be summarized by an equivalent Gaussian statistics [33–36].

- In our formulation, we excluded the effect of label noise in the training set [14] to avoid clutter, since the effect of label noise with variance  $\sigma^2$  can equivalently be studied by shifting  $\bar{\boldsymbol{\psi}}^\mu \rightarrow \bar{\boldsymbol{\psi}}^\mu + \mathbf{n}^\mu$  with an independent random vector  $\mathbf{n}$  with  $\mathbb{E}(\bar{\mathbf{w}} \cdot \mathbf{n})^2 = \sigma^2$ .
- We assume that the encoding representations depend on centers via

$$\boldsymbol{\psi}(\mathbf{x}) = \mathbf{A} \bar{\boldsymbol{\psi}}(\mathbf{x}) + \boldsymbol{\delta}(\mathbf{x}) \quad (\text{A7})$$

Here,  $\mathbf{A} \in \mathbb{R}^{M \times N}$  is a deterministic projection matrix that models the relation between centers and encoding features. The noise representation  $\boldsymbol{\delta}(\mathbf{x}) \in \mathbb{R}^M$  models the *variations* in the encoding features, and is the source of randomness in  $\boldsymbol{\psi}(\mathbf{x})$  for each fixed input  $\mathbf{x}$ .

- While, in general,  $\delta(\mathbf{x})$  should be thought of as a random feature conditioned on each input  $\mathbf{x}$ , here we consider a noise model independent of centers. The simplest model for  $\delta(\mathbf{x})$  with input correlations is a linear random feature model  $\delta(\mathbf{x}) = \mathbf{B}\psi(\mathbf{x}) + \delta_0$  where  $\mathbf{B} \in \mathbb{R}^{M \times N}$  is a random matrix, and  $\delta_0$  is a random vector which are drawn independently from their respective distributions. The study of this model requires computing another quenched average over random features  $\mathbf{B}$  and is left for future work. See [17, 37] for the analysis of a similar model in ridge regression setting.
- In particular, we will apply our theory to the case where  $\psi(\mathbf{x}) = \bar{\psi}(\mathbf{x}) + \delta$  where  $\delta \in \mathbb{R}^N$  models the variances in the inputs that are irrelevant to the target. The dimensionalities of the features  $\psi$  and  $\bar{\psi}$  are chosen to be the same for notational convenience, however, can be trivially applied to a more general setting with  $\psi = \mathbf{A}\bar{\psi} + \delta$ , since our final result will depend only on the covariance matrices in Eq. A6 and the coding direction  $\bar{\mathbf{w}}$ .

## 1. Replica Calculation

We set up a general framework for our calculation. The measure for the weights are denoted as  $d\mu(\mathbf{w})$ , and the loss function  $\ell(\mathbf{w} \cdot \psi - \bar{\mathbf{w}} \cdot \bar{\psi})$  is kept generic. Then, the partition function is given by

$$Z = \int d\tilde{\mu}(\mathbf{w}) e^{-\frac{\beta}{\lambda} \sum_{\mu=1}^P \ell(\mathbf{w} \cdot \psi^\mu - \bar{\mathbf{w}} \cdot \bar{\psi}^\mu)}, \quad d\tilde{\mu}(\mathbf{w}) \equiv d\mu(\mathbf{w}) e^{-\beta \mathbf{w}^\top \mathbf{J}_{\psi \bar{\psi}} \bar{\mathbf{w}}} \quad (\text{A8})$$

where we defined  $d\tilde{\mu}(\mathbf{w})$  by including source terms to extract the mean and variance of the optimized weights.

First, we integrate in auxiliary variables to simplify the computation:

$$H_\mu \equiv \mathbf{w} \cdot \psi^\mu - \bar{\mathbf{w}} \cdot \bar{\psi}^\mu \quad (\text{A9})$$

and get:

$$\begin{aligned} Z &= \int d\tilde{\mu}(\mathbf{w}) \prod_{\mu} dH_\mu e^{-\frac{\beta}{\lambda} \ell(H_\mu)} \delta(H_\mu - \mathbf{w} \cdot \psi^\mu + \bar{\mathbf{w}} \cdot \bar{\psi}^\mu) \\ &= \int d\tilde{\mu}(\mathbf{w}) [d\mathcal{H}_\mu] [d\hat{H}_\mu] e^{i \sum_{\mu} \hat{H}_\mu H_\mu} e^{-i \sum_{\mu} \hat{H}_\mu (\mathbf{w} \cdot \psi^\mu - \bar{\mathbf{w}} \cdot \bar{\psi}^\mu)}, \end{aligned} \quad (\text{A10})$$

where we defined  $d\mathcal{H}_\mu \equiv dH_\mu e^{-\frac{\beta}{\lambda} \ell(H_\mu)}$  and introduced the convention where  $[dx^{a,b,\dots}]$  represents product over free indices  $[dx^{a,b,\dots}] \equiv \prod_{a,b,\dots} dx^{a,b,\dots}$ . For example,  $[d\mathcal{H}_\mu] \equiv \prod_{\mu} d\mathcal{H}_\mu$  and  $[d\hat{H}_\mu] \equiv \prod_{\mu} d\hat{H}_\mu$ .

Next, we replicate the partition function to perform averages over the data distribution:

$$Z^n = \int [d\tilde{\mu}(\mathbf{w}^a)] [d\mathcal{H}_\mu^a] [d\hat{H}_\mu^a] e^{i \sum_{a,\mu} \hat{H}_\mu^a H_\mu^a} e^{-i \sum_{a,\mu} \hat{H}_\mu^a (\mathbf{w}^a \cdot \psi^\mu - \bar{\mathbf{w}} \cdot \bar{\psi}^\mu)}. \quad (\text{A11})$$

Next, we define the  $(2N)$ -dimensional feature vector  $\gamma^\mu$  and  $(2N)$ -dimensional weight vector  $\mathcal{W}^a$  as

$$\gamma^\mu = \begin{pmatrix} \psi^\mu \\ \bar{\psi}^\mu \end{pmatrix}, \quad \mathcal{W}^a = \begin{pmatrix} \mathbf{w}^a \\ -\bar{\mathbf{w}} \end{pmatrix}, \quad (\text{A12})$$

so that for each sample, we have:

$$\mathbf{w}^a \cdot \psi^\mu - \bar{\mathbf{w}} \cdot \bar{\psi}^\mu = \mathcal{W}^a \cdot \gamma^\mu. \quad (\text{A13})$$

At this point, we make the Gaussian assumption where the statistics of  $\gamma^\mu$  can be captured by its first and second moments:

$$\langle \gamma \rangle = 0, \quad \langle \gamma \gamma^\top \rangle = \begin{pmatrix} \langle \psi \psi^\top \rangle & \langle \psi \bar{\psi}^\top \rangle \\ \langle \bar{\psi} \psi^\top \rangle & \langle \bar{\psi} \bar{\psi}^\top \rangle \end{pmatrix} = \begin{pmatrix} \Sigma_{\psi}/N & \Sigma_{\psi \bar{\psi}}/N \\ \Sigma_{\bar{\psi} \psi}^\top/N & \Sigma_{\bar{\psi}}/N \end{pmatrix} \equiv \Sigma_{\mathbf{r}} \quad (\text{A14})$$

where  $\Sigma_{\mathbf{r}} \in \mathbb{R}^{(2N) \times (2N)}$  is its covariance. With this notation, the partition function simplifies to

$$Z^n = \int [d\tilde{\mu}(\mathbf{w}^a)] [d\mathcal{H}_\mu^a] [d\hat{H}_\mu^a] e^{i \sum_{a,\mu} \hat{H}_\mu^a H_\mu^a} e^{-i \sum_{a,\mu} \hat{H}_\mu^a \mathcal{W}^a \cdot \gamma^\mu} \quad (\text{A15})$$

and with the assumption that each sample  $\gamma^\mu$  is drawn i.i.d. from the normal distribution  $\mathcal{N}(0, \Sigma_\Gamma)$ , its dataset average over  $\gamma^\mu$  yields

$$\langle Z^n \rangle = \int [d\tilde{\mu}(\mathbf{w}^a)] \left[ \int [d\mathcal{H}^a][d\hat{H}^a] e^{i\sum_a \hat{H}^a H^a} \left\langle e^{-i\sum_a \hat{H}^a \mathcal{W}^a \cdot \gamma} \right\rangle_\gamma \right]^P. \quad (\text{A16})$$

We define the order parameters  $q^a = \mathcal{W}^a \cdot \gamma$  and consider their first and second moments:

$$\langle q^a \rangle = 0, \quad C^{ab} = \langle q^a q^b \rangle = \mathcal{W}^a \Sigma_\Gamma \mathcal{W}^b, \quad (\text{A17})$$

Then the quenched average over  $\gamma \sim \mathcal{N}(0, \Sigma_\Gamma)$  gives:

$$\begin{aligned} \langle Z^n \rangle &= \int [dC^{ab}][d\tilde{\mu}(\mathbf{w}^a)] \delta(C^{ab} - \mathcal{W}^a \Sigma_\Gamma \mathcal{W}^b) \left[ \int [d\mathcal{H}^a][d\hat{H}^a] e^{i\sum_a \hat{H}^a H^a} e^{-\frac{1}{2}\sum_{a,b} \hat{H}^a C^{ab} \hat{H}^a} \right]^P \\ &= \int [dC^{ab}][d\tilde{\mu}(\mathbf{w}^a)] \delta(C^{ab} - \mathcal{W}^a \Sigma_\Gamma \mathcal{W}^b) \left[ \int [d\mathcal{H}^a] e^{-\frac{1}{2}\sum_{a,b} H^a (C^{ab})^{-1} H^b - \frac{1}{2} \log \det(C^{ab})} \right]^P, \end{aligned} \quad (\text{A18})$$

where in the last line we performed the integral over  $[d\hat{H}^a]$ . Furthermore, we integrate in new variables  $\hat{C}^{ab}$  to replace the delta function:

$$\begin{aligned} \langle Z^n \rangle &= \int [dC^{ab}][d\hat{C}^{ab}][d\tilde{\mu}(\mathbf{w}^a)] e^{i\sum_{ab} \hat{C}^{ab} (C^{ab} - \mathcal{W}^a \Sigma_\Gamma \mathcal{W}^b)} \left[ \int [d\mathcal{H}^a] e^{-\frac{1}{2}\sum_{a,b} H^a (C^{ab})^{-1} H^b - \frac{1}{2} \log \det(C^{ab})} \right]^P \\ &\equiv \int [dC^{ab}][d\hat{C}^{ab}] e^{-n\frac{\beta N}{2}(G_0 + \alpha G_1)}, \end{aligned} \quad (\text{A19})$$

where

$$\begin{aligned} G_0 &= -\frac{2}{n\beta N} \log \left( \int [d\tilde{\mu}(\mathbf{w}^a)] e^{i\sum_{ab} \hat{C}^{ab} (C^{ab} - \mathcal{W}^a \Sigma_\Gamma \mathcal{W}^b)} \right), \\ [d\tilde{\mu}(\mathbf{w}^a)] &= \prod_a d\mu(\mathbf{w}^a) e^{-\beta \mathbf{w}^a \top \mathbf{J}_{\psi\bar{\psi}} \bar{\mathbf{w}}}, \\ \mathcal{W}^a &= \begin{pmatrix} \mathbf{w}^a \\ -\bar{\mathbf{w}} \end{pmatrix}, \quad \Sigma_\Gamma \equiv \frac{1}{N} \begin{pmatrix} \Sigma_\psi & \Sigma_{\psi\bar{\psi}} \\ \Sigma_{\psi\bar{\psi}}^\top & \Sigma_{\bar{\psi}} \end{pmatrix} \end{aligned} \quad (\text{A20})$$

and

$$\begin{aligned} G_1 &= -\frac{2}{n\beta} \log \left( \int [d\mathcal{H}^a] e^{-\frac{1}{2}\sum_{a,b} H^a (C^{ab})^{-1} H^b - \frac{1}{2} \log \det(C^{ab})} \right), \\ [d\mathcal{H}^a] &= \prod_a dH^a e^{-\frac{\beta}{\lambda} \ell(H^a)} \end{aligned} \quad (\text{A21})$$

The coefficients were chosen so that  $G_0$  and  $G_1$  remain  $\mathcal{O}(1)$  in the thermodynamic limit  $N \rightarrow \infty$  while  $\alpha \equiv P/N \sim \mathcal{O}(1)$ . Next, we compute these two terms under the replica symmetric ansatz:

$$\begin{aligned} \mathbf{C} &= \frac{1}{\beta} \left( Q \mathbf{I}_n + \beta C \mathbf{1}_n \mathbf{1}_n^\top \right) \\ \hat{\mathbf{C}} &= \frac{\beta N}{2i} \left( \hat{Q} \mathbf{I}_n + \beta \hat{C} \mathbf{1}_n \mathbf{1}_n^\top \right). \end{aligned} \quad (\text{A22})$$

**The  $G_0$  term:** Representing  $\mathbf{C}$  and  $\hat{\mathbf{C}}$  as  $n \times n$ -matrices with entries  $C^{ab}$  and  $\hat{C}^{ab}$ , the  $G_0$  term can be written as:

$$G_0 = -\frac{2i}{n\beta N} \text{Tr} \hat{\mathbf{C}} \mathbf{C} - \frac{2}{n\beta N} \log \left( \int [d\tilde{\mu}(\mathbf{w}^a)] e^{-i\sum_{ab} \hat{C}^{ab} \mathcal{W}^a \Sigma_\Gamma \mathcal{W}^b} \right) \quad (\text{A23})$$

Choosing  $d\mu(\mathbf{w}^a) = \left(\frac{\beta}{2\pi}\right)^{N/2} e^{-\frac{\beta}{2}\|\mathbf{w}^a\|^2}$ , the measure simplifies to

$$[d\tilde{\mu}(\mathbf{w}^a)] = \prod_a d\mu(\mathbf{w}^a) e^{-\beta \mathbf{w}^a \top \mathbf{J}_{\psi\bar{\psi}} \bar{\mathbf{w}}} = \left(\frac{\beta}{2\pi}\right)^{nN/2} \prod_a d\mathbf{w}^a e^{-\frac{\beta}{2}(\|\mathbf{w}^a\|^2 + 2\mathbf{w}^a \top \mathbf{J}_{\psi\bar{\psi}} \bar{\mathbf{w}})} \quad (\text{A24})$$



Taking the constants out:

$$G_0 = -\frac{2i}{n\beta N} \text{Tr } \hat{\mathbf{C}}\mathbf{C} - \frac{2}{n\beta N} \log I_0$$

$$I_0 \equiv \left(\frac{\beta}{2\pi}\right)^{nN/2} \int [d\mathbf{w}^a] e^{-\frac{\beta}{2} \sum_a (\|\mathbf{w}^a\|^2 + 2\mathbf{w}^{a\top} \mathbf{J}_{\psi\bar{\psi}} \bar{\mathbf{w}}) - i \sum_{a,b} \hat{C}^{ab} \mathcal{W}^a \Sigma_{\Gamma} \mathcal{W}^b}. \quad (\text{A25})$$

The integral  $I_0$  must be evaluated based on the structure of  $\Sigma_{\Gamma}$  and  $\mathcal{W}^a$  which are given above. Then the term  $\mathcal{W}^a \Sigma_{\Gamma} \mathcal{W}^b$  can be expanded as:

$$\mathcal{W}^a \Sigma_{\Gamma} \mathcal{W}^b = \mathbf{w}^a \Sigma_{\psi} \mathbf{w}^b + \bar{\mathbf{w}} \Sigma_{\bar{\psi}} \bar{\mathbf{w}} - (\mathbf{w}^a + \mathbf{w}^b) \Sigma_{\psi\bar{\psi}} \bar{\mathbf{w}} \quad (\text{A26})$$

Then, the exponent in  $I_0$  can be written in a compact form by defining:

$$\mathbf{W} = (\mathbf{w}^1 \ \mathbf{w}^2 \ \dots \ \mathbf{w}^a \ \dots \ \mathbf{w}^n)$$

$$\bar{\mathbf{W}} = (\bar{\mathbf{w}} \ \bar{\mathbf{w}} \ \dots \ \bar{\mathbf{w}} \ \dots \ \bar{\mathbf{w}}) = \bar{\mathbf{w}} \otimes \mathbf{1}_n$$

$$\mathbf{X} = \frac{2i}{\beta} \Sigma_{\psi} \otimes \hat{\mathbf{C}}, \quad \mathbf{Y} = \frac{2i}{\beta} \Sigma_{\psi\bar{\psi}} \otimes \hat{\mathbf{C}}, \quad \mathbf{Z} = \frac{2i}{\beta} \Sigma_{\bar{\psi}} \otimes \hat{\mathbf{C}}, \quad \mathbf{J} = \mathbf{J}_{\psi\bar{\psi}} \otimes \mathbf{I}_n \quad (\text{A27})$$

yielding

$$-i \sum_{a,b} \hat{C}^{ab} \mathcal{W}^a \Sigma_{\Gamma} \mathcal{W}^b = -\frac{\beta}{2} (\mathbf{W}^{\top} \mathbf{X} \mathbf{W} - 2\mathbf{W}^{\top} \mathbf{Y} \bar{\mathbf{W}} + \bar{\mathbf{W}}^{\top} \mathbf{Z} \bar{\mathbf{W}}). \quad (\text{A28})$$

Plugging this in the integral, we get

$$I_0 = \left(\frac{\beta}{2\pi}\right)^{nN/2} \int d\mathbf{W} e^{-\frac{\beta}{2} (\mathbf{W}^{\top} (\mathbf{I} + \mathbf{X}) \mathbf{W} + 2\mathbf{W}^{\top} (\mathbf{J} - \mathbf{Y}) \bar{\mathbf{W}} + \bar{\mathbf{W}}^{\top} \mathbf{Z} \bar{\mathbf{W}})}. \quad (\text{A29})$$

The measure also becomes  $[d\mathbf{w}^a] = d\mathbf{W}$  and the integral over  $nN$ -dimensional space can be simply evaluated to:

$$\log I_0 = -\frac{1}{2} \log \det(\mathbf{I} + \mathbf{X}) - \frac{\beta}{2} \bar{\mathbf{W}}^{\top} \left[ \mathbf{Z} - (\mathbf{J} - \mathbf{Y})^{\top} (\mathbf{I} + \mathbf{X})^{-1} (\mathbf{J} - \mathbf{Y}) \right] \bar{\mathbf{W}}. \quad (\text{A30})$$

Plugging in the replica symmetric ansatz  $\hat{\mathbf{C}} = \frac{\beta N}{2i} (\hat{Q} \mathbf{I}_n + \beta \hat{C} \mathbf{1}_n \mathbf{1}_n^{\top})$  (A22), matrices  $\mathbf{X}$ ,  $\mathbf{Y}$  and  $\mathbf{Z}$  simplify to

$$\begin{aligned} \mathbf{X} &= \hat{Q} \Sigma_{\psi} \otimes \mathbf{I}_n + \beta \hat{C} \Sigma_{\psi} \otimes \mathbf{1}_n \mathbf{1}_n^{\top}, \\ \mathbf{Y} &= \hat{Q} \Sigma_{\psi\bar{\psi}} \otimes \mathbf{I}_n + \beta \hat{C} \Sigma_{\psi\bar{\psi}} \otimes \mathbf{1}_n \mathbf{1}_n^{\top}, \\ \mathbf{Z} &= \hat{Q} \Sigma_{\bar{\psi}} \otimes \mathbf{I}_n + \beta \hat{C} \Sigma_{\bar{\psi}} \otimes \mathbf{1}_n \mathbf{1}_n^{\top}. \end{aligned} \quad (\text{A31})$$

The  $\log \det(\mathbf{I} + \mathbf{X})$  simplifies to

$$\begin{aligned} &\log \det \left[ (\mathbf{I}_N + \hat{Q} \Sigma_{\psi}) \otimes \mathbf{I}_n \right] + \log \det \left[ \mathbf{I} + \beta \hat{C} \Sigma_{\psi} (\mathbf{I}_N + \hat{Q} \Sigma_{\psi})^{-1} \otimes \mathbf{1}_n \mathbf{1}_n^{\top} \right] \\ &= n \log \det \mathbf{G} + \text{Tr} \log \left( \mathbf{I} + \beta \hat{C} \Sigma_{\psi} \mathbf{G}^{-1} \otimes \mathbf{1}_n \mathbf{1}_n^{\top} \right) \\ &= n\beta N \left( \frac{1}{\beta N} \log \det \mathbf{G} + \hat{C} \frac{1}{N} \text{Tr} \Sigma_{\psi} \mathbf{G}^{-1} \right) + \mathcal{O}(n^2) \end{aligned} \quad (\text{A32})$$

where we defined  $\mathbf{G} \equiv \mathbf{I}_N + \hat{Q} \Sigma_{\psi}$ , used the identity  $\log \det \mathbf{A} = \text{Tr} \log \mathbf{A}$  (second line), and Taylor expanded the log in small  $n$  (last line).

Next, we compute  $(\mathbf{I} + \mathbf{X})^{-1}$  in the limit  $n \rightarrow 0$ :

$$\begin{aligned} (\mathbf{I} + \mathbf{X})^{-1} &= \left( (\mathbf{I}_N + \hat{Q} \Sigma_{\psi})^{-1} \otimes \mathbf{I}_n \right) \left( \mathbf{I} + \beta \hat{C} \Sigma_{\psi} \mathbf{G}^{-1} \otimes \mathbf{1}_n \mathbf{1}_n^{\top} \right)^{-1} \\ &= \left( \mathbf{G}^{-1} \otimes \mathbf{I}_n \right) \left( \mathbf{I} - \beta \hat{C} \Sigma_{\psi} \mathbf{G}^{-1} \otimes \mathbf{1}_n \mathbf{1}_n^{\top} + \mathcal{O}(n) \right) \\ &= \mathbf{G}^{-1} \otimes \mathbf{I}_n - \beta \hat{C} \mathbf{G}^{-1} \Sigma_{\psi} \mathbf{G}^{-1} \otimes \mathbf{1}_n \mathbf{1}_n^{\top} + \mathcal{O}(n). \end{aligned} \quad (\text{A33})$$

Note that the second and third terms in  $\log I_0$  are of the form  $\bar{\mathbf{w}} \otimes \mathbf{1}_n(\dots)\bar{\mathbf{w}} \otimes \mathbf{1}_n$ , meaning that only terms like  $\mathbf{A} \otimes \mathbf{I}_n$  in parentheses survive in the leading order. Therefore, the second term in  $\log I_0$  becomes:

$$-\frac{n\beta}{2}\bar{\mathbf{w}}^\top \left[ \hat{Q}\Sigma_{\bar{\psi}} - \left( \mathbf{J}_{\psi\bar{\psi}} - \hat{Q}\Sigma_{\psi\bar{\psi}} \right)^\top \mathbf{G}^{-1} \left( \mathbf{J}_{\psi\bar{\psi}} - \hat{Q}\Sigma_{\psi\bar{\psi}} \right) \right] \bar{\mathbf{w}} + \mathcal{O}(n^2) \quad (\text{A34})$$

Then,  $\log I_0$  becomes

$$-\frac{2}{n\beta N} \log I_0 = \frac{1}{\beta N} \log \det \mathbf{G} + \hat{C} \text{tr} \Sigma_{\psi} \mathbf{G}^{-1} + \text{tr} \bar{\mathbf{w}} \bar{\mathbf{w}}^\top \left[ \hat{Q}\Sigma_{\bar{\psi}} - \left( \mathbf{J}_{\psi\bar{\psi}} - \hat{Q}\Sigma_{\psi\bar{\psi}} \right)^\top \mathbf{G}^{-1} \left( \mathbf{J}_{\psi\bar{\psi}} - \hat{Q}\Sigma_{\psi\bar{\psi}} \right) \right], \quad (\text{A35})$$

where we introduced the normalized trace operation

$$\text{tr} \mathbf{M} = \frac{1}{\dim \mathbf{M}} \text{Tr} \mathbf{M}. \quad (\text{A36})$$

Finally, noting that the term  $-\frac{2i}{n\beta N} \text{Tr} \hat{\mathbf{C}}\mathbf{C}$  reduces to  $-\frac{1}{\beta} Q\hat{Q} - \hat{C}Q - \hat{Q}C$ , and keeping terms up to  $\mathcal{O}(\mathbf{J}_{\psi\bar{\psi}})$ ,  $G_0$  becomes:

$$\begin{aligned} G_0 &= \frac{1}{\beta} \left( \frac{1}{N} \log \det \mathbf{G} - Q\hat{Q} \right) - \hat{C}(Q - \text{tr} \Sigma_{\psi} \mathbf{G}^{-1}) - \hat{Q} \left( C - \text{tr} \bar{\mathbf{w}} \bar{\mathbf{w}}^\top \left[ \Sigma_{\bar{\psi}} - \Sigma_{\psi\bar{\psi}}^\top \left( \hat{Q}\mathbf{G}^{-1} \right) \Sigma_{\psi\bar{\psi}} \right] \right) \\ &\quad + 2 \text{tr} \mathbf{J}_{\psi\bar{\psi}} \bar{\mathbf{w}} \bar{\mathbf{w}}^\top \Sigma_{\psi\bar{\psi}}^\top \left( \hat{Q}\mathbf{G}^{-1} \right), \\ \mathbf{G} &= \mathbf{I} + \hat{Q}N\Sigma_{\psi} \end{aligned} \quad (\text{A37})$$

At this point, we can make further simplification assuming that  $\Sigma_{\psi}$  is full-rank and using the identity

$$\hat{Q}\mathbf{G}^{-1} = (\mathbf{I} - \mathbf{G}^{-1})\Sigma_{\psi}^{-1} = \Sigma_{\psi}^{-1}(\mathbf{I} - \mathbf{G}^{-1}), \quad (\text{A38})$$

we get

$$\begin{aligned} G_0 &= -\hat{C}(Q - \text{tr} \Sigma_{\psi} \mathbf{G}^{-1}) - \hat{Q} \left( C - \text{tr} \bar{\mathbf{w}} \bar{\mathbf{w}}^\top \left( \Sigma_{\bar{\psi}} - \Sigma_{\psi\bar{\psi}}^\top \Sigma_{\psi}^{-1} \Sigma_{\psi\bar{\psi}} \right) \right) \\ &\quad + \text{tr} \bar{\mathbf{w}} \bar{\mathbf{w}}^\top \left( \Sigma_{\psi}^{-1} \Sigma_{\psi\bar{\psi}} \right)^\top (\mathbf{I} - \mathbf{G}^{-1}) \left( \Sigma_{\psi}^{-1} \Sigma_{\psi\bar{\psi}} + 2\mathbf{J}_{\psi\bar{\psi}} \right). \end{aligned} \quad (\text{A39})$$

Finally, we define the irreducible error

$$\begin{aligned} E_\infty &= \text{tr} \bar{\mathbf{w}} \bar{\mathbf{w}}^\top \Sigma_{\bar{\psi}} - \text{tr} \mathbf{w}_* \mathbf{w}_*^\top \Sigma_{\psi} \\ \mathbf{w}_* &= \Sigma_{\psi}^{-1} \Sigma_{\psi\bar{\psi}} \bar{\mathbf{w}}, \end{aligned} \quad (\text{A40})$$

where  $\mathbf{w}_*$  is the target weights projected on the learnable subspace and  $\mathbf{w}_*^\top \Sigma_{\psi} \mathbf{w}_*$  is the maximum explainable variance by the model. With these definitions, the equation for  $G_0$  finally simplifies to:

$$\begin{aligned} G_0 &= -\hat{C}(Q - \text{tr} \Sigma_{\psi} \mathbf{G}^{-1}) - \hat{Q}(C - E_\infty) + \text{tr} \mathbf{w}_* \mathbf{w}_*^\top (\mathbf{I} - \mathbf{G}^{-1}) + 2 \text{tr} \mathbf{J}_{\psi\bar{\psi}} \bar{\mathbf{w}} \mathbf{w}_*^\top (\mathbf{I} - \mathbf{G}^{-1}), \\ \mathbf{G} &= \mathbf{I} + \hat{Q}\Sigma_{\psi}, \\ \mathbf{w}_* &= \Sigma_{\psi}^{-1} \Sigma_{\psi\bar{\psi}} \bar{\mathbf{w}}, \\ E_\infty &= \text{tr} \bar{\mathbf{w}} \bar{\mathbf{w}}^\top \Sigma_{\bar{\psi}} - \text{tr} \mathbf{w}_* \mathbf{w}_*^\top \Sigma_{\psi}, \end{aligned} \quad (\text{A41})$$

**The  $G_1$  term:** The  $G_1$  term is given by

$$\begin{aligned} G_1 &= -\frac{2}{n\beta} \left( -\frac{1}{2} \log \det(\mathbf{C}) + \log I_1 \right), \\ I_1 &= \int [d\mathcal{H}^a] e^{-\frac{1}{2} \Sigma_{a,b} H^a (C^{ab})^{-1} H^b}, \quad [d\mathcal{H}^a] = \prod_a dH^a e^{-\frac{\beta}{\lambda} \ell(H^a)} \end{aligned} \quad (\text{A42})$$

Under the replica symmetric ansatz  $\mathbf{C} = \frac{1}{\beta} (Q\mathbf{I}_n + \beta C\mathbf{1}_n\mathbf{1}_n^\top)$ :

$$\begin{aligned}\log \det(\mathbf{C}) &= n \left( \log(Q/\beta) + \frac{\beta C}{Q} \right) + \mathcal{O}(n), \\ \mathbf{C}^{-1} &= \frac{\beta}{Q}\mathbf{I}_n - \frac{\beta^2 C}{Q^2}\mathbf{1}_n\mathbf{1}_n^\top + \mathcal{O}(n),\end{aligned}\tag{A43}$$

where we used the identity  $\log \det \mathbf{A} = \text{Tr} \log \mathbf{A}$  for the first expression and used the Sherman-Morrison formula for the second expression. Hence,  $I_1$  becomes

$$I_1 = \int [d\mathcal{H}^a] e^{-\frac{\beta}{2Q} \sum_a (H^a)^2 + \frac{\beta^2 C}{2Q^2} \sum_{a,b} H^a H^b}.\tag{A44}$$

Using the Hubbard-Stratonovich transformation, this integral can be written as

$$\begin{aligned}I_1(C, C_0) &= \int DT \left[ \int d\mathcal{H} e^{-\frac{\beta}{2Q} H^2 + \frac{\beta\sqrt{C}}{Q} HT} \right]^n \\ &= \int DT \left[ e^{\frac{\beta C}{2Q} T^2} \int d\mathcal{H} e^{-\frac{\beta}{2Q} (H - \sqrt{C}T)^2} \right]^n \\ &= \int DT \left[ e^{\frac{\beta C}{2Q} T^2 + \frac{1}{2} \log(Q/\beta) + \log z(T)} \right]^n,\end{aligned}\tag{A45}$$

where  $DT = \frac{dT}{\sqrt{2\pi}} e^{-T^2/2}$  is the standard Gaussian measure and we defined

$$z(T) = \int d\mathcal{H} \sqrt{\frac{\beta}{Q}} e^{-\frac{\beta}{2Q} (H - \sqrt{C}T)^2} = \int dH \sqrt{\frac{\beta C}{Q}} e^{-\frac{\beta C}{2Q} (H - T)^2 - \frac{\beta}{\lambda} \ell(H\sqrt{C})},\tag{A46}$$

where we redefined  $H \rightarrow H\sqrt{C}$ . Using  $\int DTA^n = \int DT(1 + n \log A) = 1 + n \int DT \log A$  in the limit  $n \rightarrow 0$ , we obtain:

$$\log I_1 = n \frac{\beta C}{2Q} + \frac{n}{2} \log(Q/\beta) + n \int DT \log z(T).\tag{A47}$$

Inserting this expression in  $G_1$ , we simplify

$$\begin{aligned}G_1 &= -\frac{2}{n\beta} \left( -\frac{1}{2} \log \det(\mathbf{C}) + \log I_1 \right), \\ &= \frac{1}{\beta} \log(Q/\beta) + \frac{C}{Q} - \left( \frac{C}{Q} + \frac{1}{\beta} \log(Q/\beta) + \frac{2}{\beta} \int DT \log z(T) \right) \\ &= -\frac{2}{\beta} \int DT \log z(T).\end{aligned}\tag{A48}$$

To evaluate this integral, we first express  $z(T)$  as

$$z(T) = \int dH \sqrt{\frac{\beta C}{Q}} e^{-\beta L(H)}, \quad L(H) = \frac{C}{2Q} \left[ (H - T)^2 + \frac{2Q}{\lambda C} \ell(H\sqrt{C}) \right].\tag{A49}$$

Note that as  $\beta \rightarrow \infty$ , the integral concentrates around the saddle point  $H^* = \arg \min_H L(H)$  of  $L(H)$ . Plugging this saddle point back,  $G_1$  becomes

$$G_1 = -\frac{1}{\beta} \log \left( \frac{\beta C}{Q} \right) + 2 \langle L^*(T) \rangle_T,\tag{A50}$$

where

$$L^*(T) \equiv L(H^*(T)), \quad H^*(T) = \arg \min_H \frac{C}{2Q} \left[ (H - T)^2 + \frac{2Q}{\lambda C} \ell(H\sqrt{C}) \right].\tag{A51}$$

We will consider the squared  $\varepsilon$ -insensitive loss function:

$$\ell(x) = \frac{1}{n!} \max(0, |x| - \varepsilon)^n. \quad (\text{A52})$$

Then, we have

$$L(H) = \frac{C}{2Q} \left[ (H - T)^2 + \tilde{\lambda} \frac{2}{n!} \max(0, |H| - \tilde{\varepsilon})^n \right] \quad (\text{A53})$$

where we defined the following effective quantities:

$$\tilde{\varepsilon} \equiv \frac{\varepsilon}{\sqrt{C}}, \quad \tilde{\lambda} \equiv \frac{Q}{\lambda} C^{\frac{n-2}{2}}, \quad (\text{A54})$$

where  $\tilde{\varepsilon}$  is the effective slack variable; since  $C$  is the generalization error, having  $\varepsilon^2 \gg C$  effectively corresponds to having an infinite slack variable  $\tilde{\varepsilon}$ . Similarly,  $\tilde{\lambda}$  is the effective regularization. For the following, we solve the saddle point equations for  $n = 2$ . In terms of the quantities  $\tilde{\varepsilon}$  and  $\tilde{\lambda}$ , the saddle point  $H^*(T)$  and  $L(H^*)$  are given by:

$$H^*(T) = \begin{cases} \frac{T + \tilde{\varepsilon} \tilde{\lambda}}{1 + \tilde{\lambda}}, & \tilde{\varepsilon} < T < \infty \\ T, & -\tilde{\varepsilon} < T < \tilde{\varepsilon} \\ \frac{T - \tilde{\varepsilon} \tilde{\lambda}}{1 + \tilde{\lambda}}, & -\infty < T < -\tilde{\varepsilon} \end{cases}, \quad L(H^*) = \begin{cases} \frac{C}{2Q} \frac{\tilde{\lambda}}{1 + \tilde{\lambda}} (|T| - \tilde{\varepsilon})^2, & \tilde{\varepsilon} < |T| \\ 0, & |T| < \tilde{\varepsilon} \end{cases} \quad (\text{A55})$$

Now, we can evaluate the term  $\langle L(H^*) \rangle_T$  as:

$$\begin{aligned} \langle L(H^*) \rangle_T &= \frac{2}{\sqrt{2\pi}} \int_{\tilde{\varepsilon}}^{\infty} \frac{C}{2Q} \frac{(T - \tilde{\varepsilon})^2}{1 + \tilde{\lambda}} e^{-T^2/2} dT \\ &= \frac{C}{2Q} \frac{1}{1 + \tilde{\lambda}} \sqrt{\frac{2}{\pi}} \left[ \int_{\tilde{\varepsilon}}^{\infty} (T - \tilde{\varepsilon})^2 e^{-T^2/2} dT \right]. \end{aligned} \quad (\text{A56})$$

Simplifying this in terms of error functions, we get:

$$\begin{aligned} G_1 &= \frac{C}{Q} \frac{1}{1 + \tilde{\lambda}} \left[ (1 + \tilde{\varepsilon}^2) \operatorname{erfc} \left( \frac{\tilde{\varepsilon}}{\sqrt{2}} \right) - \tilde{\varepsilon} \sqrt{\frac{2}{\pi}} e^{-\frac{\tilde{\varepsilon}^2}{2}} \right] - \frac{1}{\beta} \log \left( \frac{\beta C}{Q} \right) \\ &= \frac{C}{Q + \tilde{\lambda}} f(\tilde{\varepsilon}) g(\tilde{\varepsilon}) - \frac{1}{\beta} \log \left( \frac{\beta C}{Q} \right) \end{aligned} \quad (\text{A57})$$

where we defined the following functions for simplicity

$$f(\tilde{\varepsilon}) = \operatorname{erfc} \left( \frac{\tilde{\varepsilon}}{\sqrt{2}} \right), \quad g(\tilde{\varepsilon}) = 1 + \tilde{\varepsilon}^2 - \tilde{\varepsilon} \frac{\sqrt{\frac{2}{\pi}} e^{-\frac{\tilde{\varepsilon}^2}{2}}}{\operatorname{erfc} \left( \frac{\tilde{\varepsilon}}{\sqrt{2}} \right)} \quad (\text{A58})$$

## 2. Combining all terms

In the thermodynamic limit  $P \rightarrow \infty$ , the final partition function after the replica symmetric ansatz becomes:

$$\langle \log Z \rangle = \lim_{n \rightarrow 0} \frac{\langle Z^n \rangle - 1}{n} = -\frac{\beta N}{2} S^*, \quad (\text{A59})$$

where  $S^*$  is obtained by solving the following saddle point equation

$$\begin{aligned} S^* &= \operatorname{extr}_{c, \hat{C}, Q, \hat{Q}} \left[ G_0 + \alpha G_1 + \frac{1}{\beta} \left( \frac{1}{N} \log \det \mathbf{G} - Q \hat{Q} - \alpha \log \left( \frac{\beta C}{Q} \right) \right) \right] \\ G_0 &= -\hat{C} (Q - \operatorname{tr} \boldsymbol{\Sigma}_{\psi} \mathbf{G}^{-1}) - \hat{Q} (C - E_{\infty}) + \operatorname{tr} \left( \mathbf{w}_* + 2 \mathbf{J}_{\psi \bar{\psi}} \bar{\mathbf{w}} \right) \mathbf{w}_*^{\top} (\mathbf{I} - \mathbf{G}^{-1}), \\ G_1 &= \frac{C}{Q + \tilde{\lambda}} f(\tilde{\varepsilon}) g(\tilde{\varepsilon}), \end{aligned} \quad (\text{A60})$$

where we have the following definitions

$$\begin{aligned} E_\infty &= \text{tr } \bar{\mathbf{w}}\bar{\mathbf{w}}^\top \Sigma_{\psi\bar{\psi}} - \text{tr } \mathbf{w}_* \mathbf{w}_*^\top \Sigma_{\psi\psi}, \\ \mathbf{G} &= \mathbf{I} + \hat{Q} \Sigma_{\psi\psi}, \quad \tilde{\varepsilon} = \frac{\varepsilon}{\sqrt{C}}, \quad \mathbf{w}_* = \Sigma_{\psi\psi}^{-1} \Sigma_{\psi\bar{\psi}} \bar{\mathbf{w}} \end{aligned} \quad (\text{A61})$$

### 3. Saddle Point Equations

We next obtain the saddle point equations for  $S$ . Let us first minimize for  $\hat{C}$ :

- Minimizing with respect to  $\hat{C}$  gives  $Q = \text{tr } \Sigma_{\psi\psi} \mathbf{G}^{-1}$ .

- Minimizing with respect to  $\hat{Q}$  gives:

$$C = -\hat{C} \text{tr } \Sigma_{\psi\psi} \mathbf{G}^{-1} \Sigma_{\psi\psi} \mathbf{G}^{-1} + E_\infty + \text{tr} \left( \mathbf{w}_* + 2\mathbf{J}_{\psi\bar{\psi}} \bar{\mathbf{w}} \right) \mathbf{w}_*^\top \mathbf{G}^{-1} \Sigma_{\psi\psi} \mathbf{G}^{-1} \quad (\text{A62})$$

- Minimizing with respect to  $C$  gives

$$\hat{Q} = \frac{\alpha f(\tilde{\varepsilon})}{Q + \lambda} \quad (\text{A63})$$

- Minimizing with respect to  $Q$  gives:

$$\hat{C} = -\frac{\alpha f(\tilde{\varepsilon})}{(Q + \lambda)^2} C g(\tilde{\varepsilon}) \quad (\text{A64})$$

- As a reminder, we had the following definitions

$$\begin{aligned} f(\tilde{\varepsilon}) &= \text{erfc} \left( \frac{\tilde{\varepsilon}}{\sqrt{2}} \right), \quad g(\tilde{\varepsilon}) = 1 + \tilde{\varepsilon}^2 - \tilde{\varepsilon} \frac{\sqrt{\frac{2}{\pi}} e^{-\frac{\tilde{\varepsilon}^2}{2}}}{\text{erfc} \left( \frac{\tilde{\varepsilon}}{\sqrt{2}} \right)}, \quad \tilde{\varepsilon} = \frac{\varepsilon}{\sqrt{C}}, \\ \mathbf{G} &= \mathbf{I} + \hat{Q} \Sigma_{\psi\psi}, \quad \mathbf{w}_* = \Sigma_{\psi\psi}^{-1} \Sigma_{\psi\bar{\psi}} \bar{\mathbf{w}}, \\ E_\infty &= \text{tr } \bar{\mathbf{w}}\bar{\mathbf{w}}^\top \Sigma_{\psi\bar{\psi}} - \text{tr } \mathbf{w}_* \mathbf{w}_*^\top \Sigma_{\psi\psi} \end{aligned} \quad (\text{A65})$$

- Notice that both  $\hat{C}$  and  $\hat{Q}$  are functions of  $C$  and  $Q$ . Hence, plugging these terms in, we get two coupled self-consistent equations as above. In general, it is challenging to solve these equations analytically.
- At the saddle point, we have

$$\begin{aligned} S^* &= \text{extr}_{C, \hat{C}, Q, \hat{Q}} [G_0 + \alpha G_1] \\ G_0 &= \hat{Q} (E_\infty - C) + \text{tr} \left( \mathbf{w}_* + 2\mathbf{J}_{\psi\bar{\psi}} \bar{\mathbf{w}} \right) \mathbf{w}_*^\top (\mathbf{I} - \mathbf{G}^{-1}) \\ &= \hat{Q} \left( E_\infty + \text{tr} \left( \mathbf{w}_* + 2\mathbf{J}_{\psi\bar{\psi}} \bar{\mathbf{w}} \right) \mathbf{w}_*^\top \Sigma_{\psi\psi} \mathbf{G}^{-1} - C \right) \\ G_1 &= \frac{1}{\alpha} \hat{Q} C g(\tilde{\varepsilon}) \end{aligned} \quad (\text{A66})$$

### 4. Simplifications

Let us define the following quantities which appear in the solution

$$\begin{aligned} \tilde{\lambda} &= \lambda + \text{tr } \Sigma_{\psi\psi} \mathbf{G}^{-1}, \quad \tilde{\varepsilon} = \frac{\varepsilon}{\sqrt{C}}, \quad \tilde{\alpha} = \alpha f(\tilde{\varepsilon}), \\ \mathbf{G} &= \mathbf{I} + \frac{\tilde{\alpha}}{\tilde{\lambda}} \Sigma_{\psi\psi}, \quad \gamma = \frac{\tilde{\alpha}}{\tilde{\lambda}^2} \text{tr } \Sigma_{\psi\psi} \mathbf{G}^{-1} \Sigma_{\psi\psi} \mathbf{G}^{-1} \end{aligned} \quad (\text{A67})$$



Then the saddle point equations are compactly written as

$$\begin{aligned} Q = \tilde{\lambda} - \lambda, \quad \hat{Q} = \frac{\tilde{\alpha}}{\tilde{\lambda}}, \quad \hat{C} = -\frac{\tilde{\alpha}}{\tilde{\lambda}^2} C g(\tilde{\varepsilon}), \quad C = \frac{1}{1 - g(\tilde{\varepsilon})\gamma} \mathcal{W}(\tilde{\varepsilon}, \tilde{\lambda}) \\ \mathcal{W}(\tilde{\varepsilon}, \tilde{\lambda}) = E_\infty + \text{tr} \left( \mathbf{w}_* + 2\mathbf{J}_{\psi\bar{\psi}} \bar{\mathbf{w}} \right) \mathbf{w}_*^\top \mathbf{G}^{-1} \Sigma_\psi \mathbf{G}^{-1} \end{aligned} \quad (\text{A68})$$

In terms of these, the action becomes:

$$\begin{aligned} \langle \log Z \rangle &= -\frac{\beta N}{2} S, \\ S &= \frac{\tilde{\alpha}}{\tilde{\lambda}} \left[ C(g(\tilde{\varepsilon}) - 1) + E_\infty + \text{tr} \left( \mathbf{w}_* + 2\mathbf{J}_{\psi\bar{\psi}} \bar{\mathbf{w}} \right) \mathbf{w}_*^\top \Sigma_\psi \mathbf{G}^{-1} \right] \\ &= \frac{\tilde{\alpha}}{\tilde{\lambda}} \left[ C g(\tilde{\varepsilon})(1 - \gamma) + \frac{\tilde{\alpha}}{\tilde{\lambda}} \text{tr} \left( \mathbf{w}_* + 2\mathbf{J}_{\psi\bar{\psi}} \bar{\mathbf{w}} \right) \mathbf{w}_*^\top \Sigma_\psi \mathbf{G}^{-1} \Sigma_\psi \mathbf{G}^{-1} \right] \\ &= \frac{\tilde{\alpha}}{\tilde{\lambda}} C g(\tilde{\varepsilon})(1 - \gamma) + \text{tr} \left( \mathbf{w}_* + 2\mathbf{J}_{\psi\bar{\psi}} \bar{\mathbf{w}} \right) \mathbf{w}_*^\top \left( \mathbf{I} - \mathbf{G}^{-1} \right)^2 \end{aligned} \quad (\text{A69})$$

Note that we can compute the following average quantities :

$$\begin{aligned} -\frac{2}{N} \frac{\partial \langle \log Z \rangle}{\partial \beta} &= \left\langle \frac{1}{N} \|\mathbf{w}\|^2 + \frac{2\alpha}{\lambda} E_{tr} \right\rangle = S \\ \frac{2\lambda}{\beta N} \frac{\partial \langle \log Z \rangle}{\partial \lambda} &= \left\langle \frac{2\alpha}{\lambda} E_{tr} \right\rangle = -\lambda \frac{\partial S}{\partial \lambda}, \end{aligned} \quad (\text{A70})$$

where the average training error is defined as  $\frac{1}{P} \sum_{\mu=1}^P \ell(\mathbf{w} \cdot \psi^\mu - \bar{\mathbf{w}} \cdot \bar{\psi}^\mu)$

## 5. Computing Variations

We have two coupled self-consistent equations in the form of

$$\begin{aligned} \tilde{\lambda} &= \mathcal{F}(\tilde{\lambda}, \tilde{\varepsilon}, x) \equiv \lambda + \text{tr} \Sigma_\psi \mathbf{G}^{-1} \\ \tilde{\varepsilon} &= \mathcal{G}(\tilde{\lambda}, \tilde{\varepsilon}, x) \equiv \varepsilon \sqrt{1 - g(\tilde{\varepsilon})\gamma} \mathcal{W}(\tilde{\varepsilon}, \tilde{\lambda})^{-1/2} \\ S &= \mathcal{H}(\tilde{\lambda}, \tilde{\varepsilon}, x) \equiv \frac{\tilde{\alpha}}{\tilde{\lambda}} \left[ \frac{\varepsilon^2}{\tilde{\varepsilon}^2} (g(\tilde{\varepsilon}) - 1) + E_\infty + \text{tr} \left( \mathbf{w}_* + 2\mathbf{J}_{\psi\bar{\psi}} \bar{\mathbf{w}} \right) \mathbf{w}_*^\top \Sigma_\psi \mathbf{G}^{-1} \right] \\ \mathcal{W}(\tilde{\varepsilon}, \tilde{\lambda}) &= E_\infty + \text{tr} \left( \mathbf{w}_* + 2\mathbf{J}_{\psi\bar{\psi}} \bar{\mathbf{w}} \right) \mathbf{w}_*^\top \mathbf{G}^{-1} \Sigma_\psi \mathbf{G}^{-1} \end{aligned} \quad (\text{A71})$$

where  $x$  collectively denotes any explicit variable. Their variations with respect to  $x$ , then is given by:

$$\begin{aligned} \delta \tilde{\lambda} &= \frac{1}{1 - \partial_{\tilde{\lambda}} \mathcal{F}} (\partial_{\tilde{\varepsilon}} \mathcal{F} \delta \tilde{\varepsilon} + \partial_x \mathcal{F} \delta x) \\ \delta \tilde{\varepsilon} &= \frac{1}{1 - \partial_{\tilde{\varepsilon}} \mathcal{G}} (\partial_{\tilde{\lambda}} \mathcal{G} \delta \tilde{\lambda} + \partial_x \mathcal{G} \delta x) \\ \delta S &= \partial_{\tilde{\lambda}} \mathcal{H} \delta \tilde{\lambda} + \partial_{\tilde{\varepsilon}} \mathcal{H} \delta \tilde{\varepsilon} + \partial_x \mathcal{H} \delta x. \end{aligned} \quad (\text{A72})$$

Solving these equations, we get

$$\begin{aligned} \delta \tilde{\lambda} &= \frac{(1 - \partial_{\tilde{\varepsilon}} \mathcal{G}) \partial_x \mathcal{F} + \partial_{\tilde{\varepsilon}} \mathcal{F} \partial_x \mathcal{G}}{(1 - \partial_{\tilde{\lambda}} \mathcal{F})(1 - \partial_{\tilde{\varepsilon}} \mathcal{G}) - \partial_{\tilde{\varepsilon}} \mathcal{F} \partial_{\tilde{\lambda}} \mathcal{G}} \delta x \\ \delta \tilde{\varepsilon} &= \frac{(1 - \partial_{\tilde{\lambda}} \mathcal{F}) \partial_x \mathcal{G} + \partial_{\tilde{\lambda}} \mathcal{G} \partial_x \mathcal{F}}{(1 - \partial_{\tilde{\lambda}} \mathcal{F})(1 - \partial_{\tilde{\varepsilon}} \mathcal{G}) - \partial_{\tilde{\varepsilon}} \mathcal{F} \partial_{\tilde{\lambda}} \mathcal{G}} \delta x. \end{aligned} \quad (\text{A73})$$

We need to compute  $\partial_{\tilde{\lambda}} \mathcal{F}$ ,  $\partial_{\tilde{\varepsilon}} \mathcal{F}$ ,  $\partial_{\tilde{\lambda}} \mathcal{G}$ ,  $\partial_{\tilde{\varepsilon}} \mathcal{G}$ . First, we compute the derivatives of  $\mathcal{F}$  and  $\mathcal{H}$ :

$$\partial_{\tilde{\lambda}} \mathcal{F} = \gamma, \quad \partial_{\tilde{\varepsilon}} \mathcal{F} = -\frac{f'}{f} \tilde{\lambda} \gamma, \quad \partial_{\tilde{\lambda}} \mathcal{H} = -\frac{f}{\tilde{\lambda}^2} \frac{g(1-\gamma)}{1-g\gamma} \mathcal{W}(\tilde{\varepsilon}, \tilde{\lambda}), \quad \partial_{\tilde{\varepsilon}} \mathcal{H} = -\frac{f'}{\tilde{\lambda}} \frac{g\gamma}{1-g\gamma} \mathcal{W}(\tilde{\varepsilon}, \tilde{\lambda}). \quad (\text{A74})$$

Note that:

$$\frac{\partial_{\tilde{\varepsilon}} \mathcal{H}}{\partial_{\tilde{\lambda}} \mathcal{H}} = -\frac{\partial_{\tilde{\varepsilon}} \mathcal{F}}{1 - \partial_{\tilde{\lambda}} \mathcal{F}} = \frac{f' \tilde{\lambda}}{f} \frac{\gamma}{1 - \gamma} \quad (\text{A75})$$

Inserting the variation of  $\delta \tilde{\lambda}$ , we get the simplification:

$$\begin{aligned} \delta S &= \partial_{\tilde{\lambda}} \mathcal{H} \left( \delta \tilde{\lambda} - \frac{\partial_{\tilde{\varepsilon}} \mathcal{F}}{1 - \partial_{\tilde{\lambda}} \mathcal{F}} \delta \tilde{\varepsilon} \right) + \partial_x \mathcal{H} \delta x = \left( \frac{\partial_{\tilde{\lambda}} \mathcal{H}}{1 - \gamma} \partial_x \mathcal{F} + \partial_x \mathcal{H} \right) \delta x \\ &= \left( -\frac{fg}{\tilde{\lambda}^2} \frac{\mathcal{W}(\tilde{\varepsilon}, \tilde{\lambda})}{1 - g\gamma} \partial_x \mathcal{F} + \partial_x \mathcal{H} \right) \delta x = \left( -f(\tilde{\varepsilon})g(\tilde{\varepsilon}) \frac{C}{\tilde{\lambda}^2} \partial_x \mathcal{F} + \partial_x \mathcal{H} \right) \delta x. \end{aligned} \quad (\text{A76})$$

The observables from the action hence only depend on  $\mathcal{F}$ . This provides a huge simplification for computing first order derivatives of  $\langle \log Z \rangle$ .

## 6. Observables

Here, we compute the expected values of the observables from the partition function using our calculations above. First, we are interested in the following observables from the partition function:

$$\begin{aligned} \frac{2\alpha}{\lambda} E_{tr} &= \frac{2\lambda}{\beta N} \frac{\partial}{\partial \lambda} \langle \log Z \rangle = -\lambda \frac{\partial S}{\partial \lambda} = \frac{\tilde{\alpha}}{\tilde{\lambda}} Cg(\tilde{\varepsilon}) \frac{\lambda}{\tilde{\lambda}}, \\ \frac{1}{N} \langle \bar{\mathbf{w}} \mathbf{w}^\top \rangle &= -\frac{1}{\beta N} \frac{\partial}{\partial \mathbf{J}_{\psi \bar{\psi}}} \langle \log Z \rangle = \frac{1}{2} \frac{\partial S}{\partial \mathbf{J}_{\psi \bar{\psi}}} = \frac{\tilde{\alpha}}{\tilde{\lambda}} \bar{\mathbf{w}} \mathbf{w}_*^\top \boldsymbol{\Sigma}_{\psi} \mathbf{G}^{-1} = \frac{1}{N} \left( \mathbf{I} - \mathbf{G}^{-1} \right) \left( \boldsymbol{\Sigma}_{\psi}^{-1} \boldsymbol{\Sigma}_{\psi \bar{\psi}} \right) \bar{\mathbf{w}} \bar{\mathbf{w}}^\top \end{aligned} \quad (\text{A77})$$

From these observables we also obtain

$$\begin{aligned} \langle \mathbf{w} \rangle &= \left( \mathbf{I} - \mathbf{G}^{-1} \right) \left( \boldsymbol{\Sigma}_{\psi}^{-1} \boldsymbol{\Sigma}_{\psi \bar{\psi}} \right) \bar{\mathbf{w}} = N \frac{\tilde{\alpha}}{\tilde{\lambda}} \mathbf{G}^{-1} \boldsymbol{\Sigma}_{\psi \bar{\psi}} \bar{\mathbf{w}}, \\ \frac{1}{N} \langle \|\mathbf{w}\|^2 \rangle &= S - \frac{2\alpha}{\lambda} E_{tr} = \frac{\tilde{\alpha}}{\tilde{\lambda}} Cg(\tilde{\varepsilon}) \left( 1 - \gamma - \frac{\lambda}{\tilde{\lambda}} \right) + \frac{1}{N} \bar{\mathbf{w}}^\top \left( \boldsymbol{\Sigma}_{\psi}^{-1} \boldsymbol{\Sigma}_{\psi \bar{\psi}} \right)^\top \left( \mathbf{I} - \mathbf{G}^{-1} \right)^2 \left( \boldsymbol{\Sigma}_{\psi}^{-1} \boldsymbol{\Sigma}_{\psi \bar{\psi}} \right) \bar{\mathbf{w}}, \\ \frac{1}{N} \langle \mathbf{w} \mathbf{w}^\top \rangle - \frac{1}{N} \langle \mathbf{w} \rangle \langle \mathbf{w} \rangle^\top &= Cg(\tilde{\varepsilon}) \frac{\tilde{\alpha}}{\tilde{\lambda}^2} \mathbf{G}^{-1} \boldsymbol{\Sigma}_{\psi} \mathbf{G}^{-1} \end{aligned} \quad (\text{A78})$$

where we used the identity  $\delta \equiv 1 - \gamma - \frac{\lambda}{\tilde{\lambda}} = \frac{\text{Tr} \mathbf{G}^{-1} \boldsymbol{\Sigma}_{\psi} \mathbf{G}^{-1}}{\tilde{\lambda}}$  at the last line.

Finally, we compute generalization error as

$$\begin{aligned} E_g &= \left\langle \mathbb{E}(\mathbf{w} \cdot \boldsymbol{\psi} - \bar{\mathbf{w}} \cdot \bar{\boldsymbol{\psi}})^2 \right\rangle = \left\langle \mathbf{w}^\top \boldsymbol{\Sigma}_{\psi} \mathbf{w} \right\rangle + \left\langle \bar{\mathbf{w}}^\top \boldsymbol{\Sigma}_{\bar{\psi}} \bar{\mathbf{w}} \right\rangle - 2 \left\langle \mathbf{w}^\top \boldsymbol{\Sigma}_{\psi \bar{\psi}} \bar{\mathbf{w}} \right\rangle \\ &= Cg(\tilde{\varepsilon})\gamma + \bar{\mathbf{w}}^\top \left[ \boldsymbol{\Sigma}_{\bar{\psi}} - 2\boldsymbol{\Sigma}_{\psi \bar{\psi}}^\top \left( \mathbf{I} - \mathbf{G}^{-1} \right) \left( \boldsymbol{\Sigma}_{\psi}^{-1} \boldsymbol{\Sigma}_{\psi \bar{\psi}} \right) + \left( \boldsymbol{\Sigma}_{\psi}^{-1} \boldsymbol{\Sigma}_{\psi \bar{\psi}} \right)^\top \boldsymbol{\Sigma}_{\psi} \left( \mathbf{I} - \mathbf{G}^{-1} \right)^2 \left( \boldsymbol{\Sigma}_{\psi}^{-1} \boldsymbol{\Sigma}_{\psi \bar{\psi}} \right) \right] \bar{\mathbf{w}} \\ &= Cg(\tilde{\varepsilon})\gamma + \bar{\mathbf{w}}^\top \left[ \boldsymbol{\Sigma}_{\bar{\psi}} - \boldsymbol{\Sigma}_{\psi \bar{\psi}}^\top \left( 2\mathbf{I} - \boldsymbol{\Sigma}_{\psi}^{-1} \left( \mathbf{I} - \mathbf{G}^{-1} \right) \boldsymbol{\Sigma}_{\psi} \right) \left( \mathbf{I} - \mathbf{G}^{-1} \right) \left( \boldsymbol{\Sigma}_{\psi}^{-1} \boldsymbol{\Sigma}_{\psi \bar{\psi}} \right) \right] \bar{\mathbf{w}} \\ &= Cg(\tilde{\varepsilon})\gamma + \bar{\mathbf{w}}^\top \left[ \boldsymbol{\Sigma}_{\bar{\psi}} - \boldsymbol{\Sigma}_{\psi \bar{\psi}}^\top \left( \mathbf{I} - \mathbf{G}^{-2} \right) \left( \boldsymbol{\Sigma}_{\psi}^{-1} \boldsymbol{\Sigma}_{\psi \bar{\psi}} \right) \right] \bar{\mathbf{w}} \\ &= Cg(\tilde{\varepsilon})\gamma + \mathcal{W}(\tilde{\varepsilon}, \tilde{\lambda}) = C. \end{aligned} \quad (\text{A79})$$

## 7. Alternative Formulation in terms of Center-Variation Covariance

We consider the data model where  $\boldsymbol{\psi} = \bar{\boldsymbol{\psi}} + \boldsymbol{\delta}$  and hence

$$\begin{aligned} \boldsymbol{\Sigma}_{\psi} &= \boldsymbol{\Sigma}_{\bar{\psi}} + \boldsymbol{\Sigma}_{\boldsymbol{\delta}} + \boldsymbol{\Sigma}_{\bar{\psi} \boldsymbol{\delta}} + \boldsymbol{\Sigma}_{\bar{\psi} \boldsymbol{\delta}}^\top \\ \boldsymbol{\Sigma}_{\psi \boldsymbol{\delta}} &= \boldsymbol{\Sigma}_{\boldsymbol{\delta}} + \boldsymbol{\Sigma}_{\bar{\psi} \boldsymbol{\delta}} \\ \boldsymbol{\Sigma}_{\psi \bar{\psi}} &= \boldsymbol{\Sigma}_{\bar{\psi}} + \boldsymbol{\Sigma}_{\bar{\psi} \boldsymbol{\delta}} = \boldsymbol{\Sigma}_{\psi} - \boldsymbol{\Sigma}_{\psi \boldsymbol{\delta}}. \end{aligned} \quad (\text{A80})$$

We also note that:

$$\Sigma_{\psi\bar{\psi}}^\top \Sigma_{\psi}^{-1} \Sigma_{\psi\bar{\psi}} = \left( \mathbf{I} - \Sigma_{\psi}^{-1} \Sigma_{\psi\delta} \right)^\top \Sigma_{\psi} \left( \mathbf{I} - \Sigma_{\psi}^{-1} \Sigma_{\psi\delta} \right) \quad (\text{A81})$$

Replacing this back in generalization error

$$\begin{aligned} \mathcal{W}(\tilde{\varepsilon}, \tilde{\lambda}) &= \bar{\mathbf{W}}^\top \mathbf{G}^{-1} \Sigma_{\psi} \mathbf{G}^{-1} \bar{\mathbf{W}} + \bar{\mathbf{w}}^\top \Sigma_{\bar{\psi}} \bar{\mathbf{w}} - \bar{\mathbf{W}}^\top \Sigma_{\psi} \bar{\mathbf{W}} \\ \bar{\mathbf{W}} &= \left( \mathbf{I} - \Sigma_{\psi}^{-1} \Sigma_{\psi\delta} \right) \bar{\mathbf{w}} \end{aligned} \quad (\text{A82})$$

## Appendix B: Optimal Learning Rates

In this section, we compute the optimal learning rates both for ridge regression by solving for  $\partial_\lambda E_g = 0$ , and for  $\varepsilon$ -SVR by solving  $\partial_\varepsilon E_g = 0$  using the analytical expression we derived. Since  $E_g$  is defined through two self-consistent equations, its derivatives also have to be solved self-consistently. Hence, in order to compute optimal hyperparameters  $\lambda$  and  $\varepsilon$ , we need to compute the variations of  $\tilde{\lambda}$  and  $\tilde{\varepsilon}$ .

### 1. Computing Variations

Again we start with the two coupled self-consistent equations in the form of

$$\begin{aligned} \tilde{\lambda} &= \mathcal{F}(\tilde{\lambda}, \tilde{\varepsilon}, x) \equiv \lambda + \text{tr} \Sigma_{\psi} \mathbf{G}^{-1} \\ \tilde{\varepsilon} &= \mathcal{G}(\tilde{\lambda}, \tilde{\varepsilon}, x) \equiv \varepsilon \sqrt{1 - g(\tilde{\varepsilon})\gamma} \mathcal{W}(\tilde{\varepsilon}, \tilde{\lambda})^{-1/2} \\ \mathcal{W}(\tilde{\varepsilon}, \tilde{\lambda}) &= E_\infty + \text{tr} \mathbf{w}_* \mathbf{w}_*^\top \mathbf{G}^{-1} \Sigma_{\psi} \mathbf{G}^{-1} \end{aligned} \quad (\text{B1})$$

where  $x$  collectively denotes any explicit variable, and we omitted the terms with  $\mathbf{J}_{\psi\bar{\psi}}$ . We found earlier that the variations of  $\tilde{\lambda}$  and  $\tilde{\varepsilon}$  are given by

$$\begin{aligned} \delta \tilde{\lambda} &= \frac{(1 - \partial_{\tilde{\varepsilon}} \mathcal{G}) \partial_x \mathcal{F} + \partial_{\tilde{\varepsilon}} \mathcal{F} \partial_x \mathcal{G}}{(1 - \partial_{\tilde{\lambda}} \mathcal{F})(1 - \partial_{\tilde{\varepsilon}} \mathcal{G}) - \partial_{\tilde{\varepsilon}} \mathcal{F} \partial_{\tilde{\lambda}} \mathcal{G}} \delta x \\ \delta \tilde{\varepsilon} &= \frac{(1 - \partial_{\tilde{\lambda}} \mathcal{F}) \partial_x \mathcal{G} + \partial_{\tilde{\lambda}} \mathcal{G} \partial_x \mathcal{F}}{(1 - \partial_{\tilde{\lambda}} \mathcal{F})(1 - \partial_{\tilde{\varepsilon}} \mathcal{G}) - \partial_{\tilde{\varepsilon}} \mathcal{F} \partial_{\tilde{\lambda}} \mathcal{G}} \delta x. \end{aligned} \quad (\text{B2})$$

and that the derivatives  $\partial_{\tilde{\lambda}} \mathcal{F}$  and  $\partial_{\tilde{\varepsilon}} \mathcal{F}$  are given by:

$$\partial_{\tilde{\lambda}} \mathcal{F} = \gamma, \quad \partial_{\tilde{\varepsilon}} \mathcal{F} = -\frac{f'}{f} \tilde{\lambda} \gamma. \quad (\text{B3})$$

Next, we compute the derivative  $\partial_{\tilde{\varepsilon}} \mathcal{G}$

$$\begin{aligned} \partial_{\tilde{\varepsilon}} \log \mathcal{G} &= -\frac{\partial_{\tilde{\varepsilon}}(g(\tilde{\varepsilon})\gamma)}{2(1 - g(\tilde{\varepsilon})\gamma)} - \frac{1}{2} \frac{\partial_{\tilde{\varepsilon}} \mathcal{W}(\tilde{\varepsilon}, \tilde{\lambda})}{\mathcal{W}(\tilde{\varepsilon}, \tilde{\lambda})} = -\frac{1}{2(1 - g(\tilde{\varepsilon})\gamma)} \left[ \partial_{\tilde{\varepsilon}}(g(\tilde{\varepsilon})\gamma) + \frac{\partial_{\tilde{\varepsilon}} \mathcal{W}(\tilde{\varepsilon}, \tilde{\lambda})}{C} \right] \\ &= -\frac{1}{2(1 - g(\tilde{\varepsilon})\gamma)} \left[ \gamma \frac{\partial_{\tilde{\varepsilon}}(f(\tilde{\varepsilon})g(\tilde{\varepsilon}))}{f(\tilde{\varepsilon})} + f(\tilde{\varepsilon})g(\tilde{\varepsilon}) \partial_{\tilde{\varepsilon}} \frac{\gamma}{f(\tilde{\varepsilon})} + \frac{\partial_{\tilde{\varepsilon}} \mathcal{W}(\tilde{\varepsilon}, \tilde{\lambda})}{C} \right]. \end{aligned} \quad (\text{B4})$$

Here,

$$\begin{aligned} \frac{\partial_{\tilde{\varepsilon}}(f(\tilde{\varepsilon})g(\tilde{\varepsilon}))}{f(\tilde{\varepsilon})} &= -\frac{2(1 - g(\tilde{\varepsilon}))}{\tilde{\varepsilon}}, & \partial_{\tilde{\varepsilon}} \frac{\gamma}{f(\tilde{\varepsilon})} &= -\frac{2\gamma}{\tilde{\varepsilon}} \frac{f' \tilde{\varepsilon}}{f^2} \frac{\tilde{\alpha}}{\tilde{\lambda}} \frac{\text{Tr} \mathbf{M}^3}{\text{Tr} \mathbf{M}^2}, \\ \partial_{\tilde{\varepsilon}} \mathcal{W}(\tilde{\varepsilon}, \tilde{\lambda}) &= -2 \text{tr} \mathbf{w}_* \mathbf{w}_*^\top \mathbf{G}^{-1} \Sigma_{\psi} \mathbf{G}^{-1} (\partial_{\tilde{\varepsilon}} \mathbf{G}) \mathbf{G}^{-1}, & \partial_{\tilde{\varepsilon}} \mathbf{G} &= \frac{f'}{f} \frac{\tilde{\alpha}}{\tilde{\lambda}} \Sigma_{\psi}, \end{aligned} \quad (\text{B5})$$

where we defined  $\mathbf{M} \equiv \boldsymbol{\Sigma}_\psi \mathbf{G}^{-1}$  to shorten the notation. Inserting these back,

$$\begin{aligned}
\tilde{\varepsilon} \partial_{\tilde{\varepsilon}} \log \mathcal{G} &= -\frac{\tilde{\varepsilon}}{2(1-g(\tilde{\varepsilon})\gamma)} \left[ -\frac{2\gamma(1-g(\tilde{\varepsilon}))}{\tilde{\varepsilon}} - \frac{2\gamma g(\tilde{\varepsilon})}{\tilde{\varepsilon}} \frac{f' \tilde{\varepsilon}}{f} \frac{\tilde{\alpha}}{\tilde{\lambda}} \frac{\text{tr} \mathbf{M}^3}{\text{tr} \mathbf{M}^2} - \frac{2}{\tilde{\varepsilon}} \frac{f' \tilde{\varepsilon}}{f} \frac{\tilde{\alpha}}{\tilde{\lambda}} \frac{\text{tr} \mathbf{M}^2 \mathbf{G}^{-1} \mathbf{w}_* \mathbf{w}_*^\top}{C} \right] \\
&= \frac{1}{(1-g(\tilde{\varepsilon})\gamma)} \left[ \gamma(1-g(\tilde{\varepsilon})) + \frac{f' \tilde{\varepsilon}}{f} \frac{\tilde{\alpha}}{\tilde{\lambda}} \left( \gamma g(\tilde{\varepsilon}) \frac{\text{tr} \mathbf{M}^3}{\text{tr} \mathbf{M}^2} + \frac{\text{tr} \mathbf{M}^2 \mathbf{G}^{-1} \mathbf{w}_* \mathbf{w}_*^\top}{C} \right) \right] \\
&= \frac{\gamma(1-g(\tilde{\varepsilon}))}{(1-g(\tilde{\varepsilon})\gamma)} + \frac{f' \tilde{\varepsilon}}{f} \frac{\tilde{\alpha}}{\tilde{\lambda}} \left( \frac{\gamma g(\tilde{\varepsilon})}{(1-g(\tilde{\varepsilon})\gamma)} \frac{\text{tr} \mathbf{M}^3}{\text{tr} \mathbf{M}^2} + \frac{\text{tr} \mathbf{M}^2 \mathbf{G}^{-1} \mathbf{w}_* \mathbf{w}_*^\top}{(1-g(\tilde{\varepsilon})\gamma)C} \right) \\
&= 1 - \frac{1-\gamma}{(1-g(\tilde{\varepsilon})\gamma)} + \frac{f' \tilde{\varepsilon}}{f} \frac{\tilde{\alpha}}{\tilde{\lambda}} \left( \frac{\gamma g(\tilde{\varepsilon})}{(1-g(\tilde{\varepsilon})\gamma)} \frac{\text{tr} \mathbf{M}^3}{\text{tr} \mathbf{M}^2} + \frac{\text{tr} \mathbf{M}^2 \mathbf{G}^{-1} \mathbf{w}_* \mathbf{w}_*^\top}{\mathcal{W}(\tilde{\varepsilon}, \tilde{\lambda})} \right)
\end{aligned} \tag{B6}$$

Since  $\partial_{\tilde{\varepsilon}} \log \mathcal{G} = \frac{\partial_{\tilde{\varepsilon}} \mathcal{G}}{\mathcal{G}} = \frac{\partial_{\tilde{\varepsilon}} \mathcal{G}}{\tilde{\varepsilon}}$ , we get:

$$\boxed{\partial_{\tilde{\varepsilon}} \mathcal{G} = \frac{\gamma(1-g(\tilde{\varepsilon}))}{(1-g(\tilde{\varepsilon})\gamma)} + \frac{f' \tilde{\varepsilon}}{f} \frac{\tilde{\alpha}}{\tilde{\lambda}} \left( \frac{\gamma g(\tilde{\varepsilon})}{(1-g(\tilde{\varepsilon})\gamma)} \frac{\text{tr} \mathbf{M}^3}{\text{tr} \mathbf{M}^2} + \frac{\text{tr} \mathbf{M}^2 \mathbf{G}^{-1} \mathbf{w}_* \mathbf{w}_*^\top}{\mathcal{W}(\tilde{\varepsilon}, \tilde{\lambda})} \right)} \tag{B7}$$

Next, we compute the derivative  $\partial_{\tilde{\lambda}} \mathcal{G}$

$$\partial_{\tilde{\lambda}} \log \mathcal{G} = -\frac{\partial_{\tilde{\lambda}}(g(\tilde{\varepsilon})\gamma)}{2(1-g(\tilde{\varepsilon})\gamma)} - \frac{1}{2} \frac{\partial_{\tilde{\lambda}} \mathcal{W}(\tilde{\varepsilon}, \tilde{\lambda})}{\mathcal{W}(\tilde{\varepsilon}, \tilde{\lambda})} = -\frac{1}{2(1-g(\tilde{\varepsilon})\gamma)} \left[ g(\tilde{\varepsilon}) \partial_{\tilde{\lambda}} \gamma + \frac{\partial_{\tilde{\lambda}} \mathcal{W}(\tilde{\varepsilon}, \tilde{\lambda})}{C} \right] \tag{B8}$$

Here, we get

$$\partial_{\tilde{\lambda}} \gamma = -\frac{2\gamma}{\tilde{\lambda}} \left( 1 - \frac{\tilde{\alpha} \text{tr} \mathbf{M}^3}{\tilde{\lambda} \text{tr} \mathbf{M}^2} \right), \quad \partial_{\tilde{\lambda}} \mathcal{W}(\tilde{\varepsilon}, \tilde{\lambda}) = -2 \text{tr} \mathbf{w}_* \mathbf{w}_*^\top \mathbf{G}^{-1} \boldsymbol{\Sigma}_\psi \mathbf{G}^{-1} (\partial_{\tilde{\lambda}} \mathbf{G}) \mathbf{G}^{-1}, \quad \partial_{\tilde{\lambda}} \mathbf{G} = -\frac{\tilde{\alpha}}{\tilde{\lambda}^2} \boldsymbol{\Sigma}_\psi. \tag{B9}$$

Inserting these

$$\begin{aligned}
\tilde{\lambda} \partial_{\tilde{\lambda}} \log \mathcal{G} &= -\frac{\tilde{\lambda}}{2(1-g(\tilde{\varepsilon})\gamma)} \left[ -\frac{2g(\tilde{\varepsilon})\gamma}{\tilde{\lambda}} \left( 1 - \frac{\tilde{\alpha} \text{tr} \mathbf{M}^3}{\tilde{\lambda} \text{tr} \mathbf{M}^2} \right) + \frac{2\tilde{\alpha} \text{tr} \mathbf{M}^2 \mathbf{G}^{-1} \mathbf{w}_* \mathbf{w}_*^\top}{\tilde{\lambda}^2 C} \right] \\
&= -\frac{1}{(1-g(\tilde{\varepsilon})\gamma)} \left[ -g(\tilde{\varepsilon})\gamma + \frac{\tilde{\alpha}}{\tilde{\lambda}} \left( g(\tilde{\varepsilon})\gamma \frac{\text{tr} \mathbf{M}^3}{\text{tr} \mathbf{M}^2} + \frac{\text{tr} \mathbf{M}^2 \mathbf{G}^{-1} \mathbf{w}_* \mathbf{w}_*^\top}{C} \right) \right] \\
&= \frac{g(\tilde{\varepsilon})\gamma}{(1-g(\tilde{\varepsilon})\gamma)} - \frac{\tilde{\alpha}}{\tilde{\lambda}} \left( \frac{g(\tilde{\varepsilon})\gamma}{(1-g(\tilde{\varepsilon})\gamma)} \frac{\text{tr} \mathbf{M}^3}{\text{tr} \mathbf{M}^2} + \frac{\text{tr} \mathbf{M}^2 \mathbf{G}^{-1} \mathbf{w}_* \mathbf{w}_*^\top}{\mathcal{W}(\tilde{\varepsilon}, \tilde{\lambda})} \right)
\end{aligned} \tag{B10}$$

Hence, we have

$$\boxed{\partial_{\tilde{\lambda}} \mathcal{G} = \frac{\tilde{\varepsilon}}{\tilde{\lambda}} \left( \frac{g(\tilde{\varepsilon})\gamma}{(1-g(\tilde{\varepsilon})\gamma)} - \frac{\tilde{\alpha}}{\tilde{\lambda}} \left( \frac{g(\tilde{\varepsilon})\gamma}{(1-g(\tilde{\varepsilon})\gamma)} \frac{\text{tr} \mathbf{M}^3}{\text{tr} \mathbf{M}^2} + \frac{\text{tr} \mathbf{M}^2 \mathbf{G}^{-1} \mathbf{w}_* \mathbf{w}_*^\top}{\mathcal{W}(\tilde{\varepsilon}, \tilde{\lambda})} \right) \right)}. \tag{B11}$$

Let us focus on the following term

$$\begin{aligned}
\frac{\tilde{\alpha}}{\tilde{\lambda}} \left( \frac{g(\tilde{\varepsilon})\gamma}{(1-g(\tilde{\varepsilon})\gamma)} \frac{\text{tr} \mathbf{M}^3}{\text{tr} \mathbf{M}^2} + \frac{\text{tr} \mathbf{M}^2 \mathbf{G}^{-1} \mathbf{w}_* \mathbf{w}_*^\top}{\mathcal{W}(\tilde{\varepsilon}, \tilde{\lambda})} \right) &= \frac{g(\tilde{\varepsilon})\gamma}{(1-g(\tilde{\varepsilon})\gamma)} \frac{\text{tr} \mathbf{M}^2 (\mathbf{I} - \mathbf{G}^{-1})}{\text{tr} \mathbf{M}^2} + \frac{\tilde{\alpha}}{\tilde{\lambda}} \frac{\text{tr} \mathbf{M}^2 \mathbf{G}^{-1} \mathbf{w}_* \mathbf{w}_*^\top}{\mathcal{W}(\tilde{\varepsilon}, \tilde{\lambda})} \\
&= \frac{g(\tilde{\varepsilon})\gamma}{(1-g(\tilde{\varepsilon})\gamma)} - \left( \frac{g(\tilde{\varepsilon})\gamma}{(1-g(\tilde{\varepsilon})\gamma)} \frac{\text{tr} \mathbf{M}^2 \mathbf{G}^{-1}}{\text{tr} \mathbf{M}^2} - \frac{\tilde{\alpha}}{\tilde{\lambda}} \frac{\text{tr} \mathbf{M}^2 \mathbf{G}^{-1} \mathbf{w}_* \mathbf{w}_*^\top}{\mathcal{W}(\tilde{\varepsilon}, \tilde{\lambda})} \right) \\
&= \frac{g(\tilde{\varepsilon})\gamma}{(1-g(\tilde{\varepsilon})\gamma)} - \frac{\gamma}{(1-g(\tilde{\varepsilon})\gamma)} \mathcal{A}(\tilde{\varepsilon}, \tilde{\lambda})
\end{aligned} \tag{B12}$$

where we defined.

$$\begin{aligned}\mathcal{A}(\tilde{\varepsilon}, \tilde{\lambda}) &= g(\tilde{\varepsilon}) \frac{\text{tr} \mathbf{M}^2 \mathbf{G}^{-1}}{\text{tr} \mathbf{M}^2} - \frac{\tilde{\lambda}}{C} \frac{\text{tr} \mathbf{M}^2 \mathbf{G}^{-1} \mathbf{w}_* \mathbf{w}_*^\top}{\text{tr} \mathbf{M}^2} \\ &= \frac{\text{tr} \mathbf{M}^2 \mathbf{G}^{-1}}{\text{tr} \mathbf{M}^2} \left( g(\tilde{\varepsilon}) - \frac{\tilde{\lambda}}{C} \frac{\text{tr} \mathbf{M}^2 \mathbf{G}^{-1} \mathbf{w}_* \mathbf{w}_*^\top}{\text{tr} \mathbf{M}^2 \mathbf{G}^{-1}} \right)\end{aligned}\quad (\text{B13})$$

This conveniently simplifies  $\partial_{\tilde{\lambda}} \mathcal{G}$  to:

$$\partial_{\tilde{\lambda}} \mathcal{G} = \frac{\tilde{\varepsilon}}{\tilde{\lambda}} \frac{\gamma}{(1 - g(\tilde{\varepsilon})\gamma)} \mathcal{A}(\tilde{\varepsilon}, \tilde{\lambda}) \quad (\text{B14})$$

Similarly,  $\partial_{\tilde{\varepsilon}} \mathcal{G}$  becomes:

$$\begin{aligned}\partial_{\tilde{\varepsilon}} \mathcal{G} &= \frac{\gamma(1 - g(\tilde{\varepsilon}))}{(1 - g(\tilde{\varepsilon})\gamma)} + \frac{f'\tilde{\varepsilon}}{f} \frac{g(\tilde{\varepsilon})\gamma}{(1 - g(\tilde{\varepsilon})\gamma)} - \frac{f'\tilde{\varepsilon}}{f} \frac{\gamma}{(1 - g(\tilde{\varepsilon})\gamma)} \mathcal{A}(\tilde{\varepsilon}, \tilde{\lambda}) \\ &= \frac{f'\tilde{\varepsilon}}{f} \frac{\gamma}{(1 - g(\tilde{\varepsilon})\gamma)} \left( \frac{f}{f'\tilde{\varepsilon}} (1 - g(\tilde{\varepsilon})) + g(\tilde{\varepsilon}) - \mathcal{A}(\tilde{\varepsilon}, \tilde{\lambda}) \right)\end{aligned}\quad (\text{B15})$$

Using the identity

$$g = 1 + \tilde{\varepsilon}^2 + \frac{f'\tilde{\varepsilon}}{f}, \quad (\text{B16})$$

this simplifies  $\partial_{\tilde{\varepsilon}} \mathcal{G}$  to

$$\partial_{\tilde{\varepsilon}} \mathcal{G} = \frac{f'\tilde{\varepsilon}}{f} \frac{\gamma}{(1 - g(\tilde{\varepsilon})\gamma)} \left[ h(\tilde{\varepsilon}) - \mathcal{A}(\tilde{\varepsilon}, \tilde{\lambda}) \right] \quad (\text{B17})$$

where we defined the function

$$h(\tilde{\varepsilon}) \equiv \tilde{\varepsilon} \left( \tilde{\varepsilon} + \frac{f'}{f} - \frac{f}{f'} \right) = \frac{(g(\tilde{\varepsilon}) - 1)^2 - g(\tilde{\varepsilon})\tilde{\varepsilon}^2}{g(\tilde{\varepsilon}) - 1 - \tilde{\varepsilon}^2}. \quad (\text{B18})$$

We obtain the denominator in Eq. B2 as

$$1 - \partial_{\tilde{\varepsilon}} \mathcal{G} - \frac{\partial_{\tilde{\varepsilon}} \mathcal{F} \partial_{\tilde{\lambda}} \mathcal{G}}{1 - \partial_{\tilde{\lambda}} \mathcal{F}} = 1 - \frac{f'\tilde{\varepsilon}}{f} \frac{\gamma}{(1 - g(\tilde{\varepsilon})\gamma)} \left[ h(\tilde{\varepsilon}) - \frac{\mathcal{A}(\tilde{\varepsilon}, \tilde{\lambda})}{1 - \gamma} \right], \quad (\text{B19})$$

Finally we get the variation of  $\tilde{\varepsilon}$  as

$$\delta \tilde{\varepsilon} = \frac{\partial_x \mathcal{G}}{1 - \partial_{\tilde{\varepsilon}} \mathcal{G} - \frac{\partial_{\tilde{\varepsilon}} \mathcal{F} \partial_{\tilde{\lambda}} \mathcal{G}}{1 - \partial_{\tilde{\lambda}} \mathcal{F}}} \delta x + \frac{\frac{\partial_{\tilde{\lambda}} \mathcal{G}}{1 - \partial_{\tilde{\lambda}} \mathcal{F}} \partial_x \mathcal{F}}{1 - \partial_{\tilde{\varepsilon}} \mathcal{G} - \frac{\partial_{\tilde{\varepsilon}} \mathcal{F} \partial_{\tilde{\lambda}} \mathcal{G}}{1 - \partial_{\tilde{\lambda}} \mathcal{F}}} \delta x \quad (\text{B20})$$

## 2. Optimal Ridge Parameter

In order to compute the optimal ridge parameter, we need to compute the derivative of generalization error  $C$  with respect to  $\lambda$  when the tube size is zero. Since

$$\partial_{\lambda} C = -2C \partial_{\lambda} \log \tilde{\varepsilon}, \quad (\text{B21})$$

it suffices to compute  $\partial_{\lambda} \tilde{\varepsilon}$  using Eq. B20

$$\partial_{\lambda} \log \tilde{\varepsilon} = \frac{1}{1 - \frac{f'\tilde{\varepsilon}}{f} \frac{\gamma}{(1 - g(\tilde{\varepsilon})\gamma)} \left[ h(\tilde{\varepsilon}) - \frac{\mathcal{A}(\tilde{\varepsilon}, \tilde{\lambda})}{1 - \gamma} \right]} \frac{1}{\tilde{\lambda}} \frac{\gamma}{(1 - g(\tilde{\varepsilon})\gamma)} \mathcal{A}(\tilde{\varepsilon}, \tilde{\lambda}) = \frac{1}{\tilde{\lambda}} \frac{\gamma}{(1 - \gamma)} \mathcal{A}(\tilde{\varepsilon}, \tilde{\lambda}), \quad (\text{B22})$$



where we used the fact that  $\varepsilon = 0$  in the last equality. Hence, the condition for optimal ridge becomes

$$\partial_\lambda C = -\frac{2C}{\tilde{\lambda}} \frac{\gamma}{(1-\gamma)} \mathcal{A}(\tilde{\varepsilon}, \tilde{\lambda}) = 0, \quad (\text{B23})$$

which implies another self-consistent equation for effective ridge parameter

$$\tilde{\lambda}_{opt} = C \frac{\text{tr} \mathbf{M}^2 \mathbf{G}^{-1}}{\text{tr} \mathbf{M}^2 \mathbf{G}^{-1} \mathbf{w}_* \mathbf{w}_*^\top} \quad (\text{B24})$$

replacing the original equation  $\tilde{\lambda} = \lambda + \text{tr} \mathbf{M}$ .

### 3. Optimal Tube Size

For optimal SVR, we set  $\lambda = 0$  and consider the derivative of generalization error with respect to  $\varepsilon$ :

$$\partial_\varepsilon C = \frac{2C}{\varepsilon} - 2C \partial_\varepsilon \log \tilde{\varepsilon}, \quad (\text{B25})$$

where  $\partial_\varepsilon \log \tilde{\varepsilon}$  is given by (Eq. B20)

$$\partial_\varepsilon \log \tilde{\varepsilon} = \frac{1}{\varepsilon} \frac{1}{1 - \frac{f' \tilde{\varepsilon}}{f} \frac{\gamma}{(1-g(\tilde{\varepsilon})\gamma)} \left[ h(\tilde{\varepsilon}) - \frac{\mathcal{A}(\tilde{\varepsilon}, \tilde{\lambda})}{1-\gamma} \right]}, \quad (\text{B26})$$

yielding

$$\partial_\varepsilon C = -2\sqrt{C} \frac{f'}{f} \frac{\gamma}{(1-g(\tilde{\varepsilon})\gamma)} \frac{\left[ h(\tilde{\varepsilon}) - \frac{\mathcal{A}(\tilde{\varepsilon}, \tilde{\lambda})}{1-\gamma} \right]}{1 - \frac{f' \tilde{\varepsilon}}{f} \frac{\gamma}{(1-g(\tilde{\varepsilon})\gamma)} \left[ h(\tilde{\varepsilon}) - \frac{\mathcal{A}(\tilde{\varepsilon}, \tilde{\lambda})}{1-\gamma} \right]} = 0. \quad (\text{B27})$$

This implies the self-consistency condition for effective tube size

$$h(\tilde{\varepsilon}_{opt}) = \frac{\mathcal{A}(\tilde{\varepsilon}_{opt}, \tilde{\lambda})}{1-\gamma}, \quad (\text{B28})$$

complemented with the self-consistent equation  $\tilde{\lambda} = \text{tr} \mathbf{M}$ .

### Appendix C: Toy Data Model

In order to analyze our result, we consider a toy data model where the center and noise model are given by

$$\begin{aligned} \boldsymbol{\psi} &= \bar{\boldsymbol{\psi}} + \sigma \boldsymbol{\delta} \\ \bar{\boldsymbol{\psi}} &\sim \mathcal{N}(0, \mathbf{I}), \quad \boldsymbol{\delta} \sim \mathcal{N}(0, \boldsymbol{\Sigma}_\delta) \\ \boldsymbol{\Sigma}_\delta &= (1-\beta) \mathbf{P} + \beta (\mathbf{I} - \mathbf{P}) = (1-\beta) \mathbf{I} + (2\beta-1) (\mathbf{I} - \mathbf{P}), \end{aligned} \quad (\text{C1})$$

where  $\mathbf{P} = \mathbf{I} - \frac{1}{N} \bar{\mathbf{w}} \bar{\mathbf{w}}^\top$  is the projection matrix to the subspace orthogonal to the coding direction. Here, we assumed that the target weights are normalized such that

$$\text{Tr} \bar{\mathbf{w}} \bar{\mathbf{w}}^\top = \text{Tr} \bar{\mathbf{w}} \bar{\mathbf{w}}^\top \boldsymbol{\Sigma}_{\bar{\boldsymbol{\psi}}} = \frac{1}{1+\beta\sigma^2} \text{Tr} \bar{\mathbf{w}} \bar{\mathbf{w}}^\top \boldsymbol{\Sigma}_\psi = N \quad (\text{C2})$$

In this model, the noise features  $\boldsymbol{\delta}$  are independent of centers  $\bar{\boldsymbol{\psi}}$ , but their covariance is allowed to correlate with the coding direction  $\bar{\mathbf{w}}$ . In this case, we get the following covariance matrices:

$$\begin{aligned} \boldsymbol{\Sigma}_{\bar{\boldsymbol{\psi}}} &= \boldsymbol{\Sigma}_{\boldsymbol{\psi} \bar{\boldsymbol{\psi}}} = \mathbf{I}, \\ \boldsymbol{\Sigma}_\psi &= \boldsymbol{\Sigma}_{\bar{\boldsymbol{\psi}}} + \sigma^2 \boldsymbol{\Sigma}_\delta = \left(1 + \sigma^2(1-\beta)\right) \mathbf{I} + \sigma^2(2\beta-1) \frac{1}{N} \bar{\mathbf{w}} \bar{\mathbf{w}}^\top. \end{aligned} \quad (\text{C3})$$

Cleaning the last expression, we get  $\Sigma_\psi$  and its inverse as:

$$\begin{aligned}\Sigma_\psi &= \left(1 + \sigma^2(1 - \beta)\right) \mathbf{P} + \left(1 + \beta\sigma^2\right) (\mathbf{I} - \mathbf{P}), \\ \Sigma_\psi^{-1} &= \frac{1}{1 + \sigma^2(1 - \beta)} \mathbf{P} + \frac{1}{1 + \beta\sigma^2} (\mathbf{I} - \mathbf{P})\end{aligned}\quad (\text{C4})$$

Hence the error at infinity becomes

$$E_\infty = \text{tr } \bar{\mathbf{w}} \bar{\mathbf{w}}^\top \left( \Sigma_{\bar{\psi}} - \Sigma_{\bar{\psi}}^\top \Sigma_\psi^{-1} \Sigma_{\psi \bar{\psi}} \right) = \frac{\beta\sigma^2}{1 + \beta\sigma^2} \quad (\text{C5})$$

We also compute  $\mathbf{G}$  and  $\mathbf{G}^{-1}$  as:

$$\begin{aligned}\mathbf{G} &= \left[ 1 + \frac{\tilde{\alpha}}{\tilde{\lambda}} \left( 1 + \sigma^2(1 - \beta) \right) \right] \mathbf{P} + \left[ 1 + \frac{\tilde{\alpha}}{\tilde{\lambda}} \left( 1 + \beta\sigma^2 \right) \right] (\mathbf{I} - \mathbf{P}) \\ \mathbf{G}^{-1} &= \frac{1}{1 + \frac{\tilde{\alpha}}{\tilde{\lambda}} \left( 1 + \sigma^2(1 - \beta) \right)} \mathbf{P} + \frac{1}{1 + \frac{\tilde{\alpha}}{\tilde{\lambda}} \left( 1 + \beta\sigma^2 \right)} (\mathbf{I} - \mathbf{P})\end{aligned}\quad (\text{C6})$$

Plugging these into our formula we get:

$$\begin{aligned}\mathcal{F}(\tilde{\lambda}, \tilde{\varepsilon}) &= \lambda + \frac{1 + \sigma^2(1 - \beta)}{1 + \frac{\tilde{\alpha}}{\tilde{\lambda}} \left( 1 + \sigma^2(1 - \beta) \right)} + \frac{1}{N} \left( \frac{1 + \beta\sigma^2}{1 + \frac{\tilde{\alpha}}{\tilde{\lambda}} \left( 1 + \beta\sigma^2 \right)} - \frac{1 + \sigma^2(1 - \beta)}{1 + \frac{\tilde{\alpha}}{\tilde{\lambda}} \left( 1 + \sigma^2(1 - \beta) \right)} \right), \\ \mathcal{G}(\tilde{\lambda}, \tilde{\varepsilon}) &= \frac{1}{1 - g(\tilde{\varepsilon})\gamma} \left( \frac{\beta\sigma^2}{1 + \beta\sigma^2} + \frac{1}{1 + \beta\sigma^2} \frac{1}{\left( 1 + \frac{\tilde{\alpha}}{\tilde{\lambda}} \left( 1 + \beta\sigma^2 \right) \right)^2} \right), \\ \gamma &= \frac{\tilde{\alpha}}{\tilde{\lambda}^2} \frac{\left( 1 + \sigma^2(1 - \beta) \right)^2}{\left( 1 + \frac{\tilde{\alpha}}{\tilde{\lambda}} \left( 1 + \sigma^2(1 - \beta) \right) \right)^2} + \frac{1}{N} \frac{\tilde{\alpha}}{\tilde{\lambda}^2} \left( \frac{\left( 1 + \beta\sigma^2 \right)^2}{\left( 1 + \frac{\tilde{\alpha}}{\tilde{\lambda}} \left( 1 + \beta\sigma^2 \right) \right)^2} - \frac{\left( 1 + \sigma^2(1 - \beta) \right)^2}{\left( 1 + \frac{\tilde{\alpha}}{\tilde{\lambda}} \left( 1 + \sigma^2(1 - \beta) \right) \right)^2} \right).\end{aligned}\quad (\text{C7})$$

For  $N \gg 1$ , we can ignore  $\mathcal{O}(N^{-1})$  terms. Furthermore, we redefine  $\tilde{\lambda} \rightarrow \frac{\tilde{\lambda}}{1 + \sigma^2(1 - \beta)}$  to simplify the self-consistent equations and obtain:

$$\begin{aligned}\mathcal{F}(\tilde{\lambda}, \tilde{\varepsilon}) &= \frac{\lambda}{1 + \sigma^2(1 - \beta)} + \frac{\tilde{\lambda}}{\tilde{\alpha} + \tilde{\lambda}}, \\ \mathcal{G}(\tilde{\lambda}, \tilde{\varepsilon}) &= \frac{1}{1 - g(\tilde{\varepsilon})\gamma} \left( \frac{\beta\sigma^2}{1 + \beta\sigma^2} + \frac{1}{1 + \beta\sigma^2} \frac{\tilde{\lambda}^2}{\left( \tilde{\lambda} + \tilde{\alpha} \frac{1 + \sigma^2\beta}{1 + \sigma^2(1 - \beta)} \right)^2} \right), \\ \gamma &= \frac{\tilde{\alpha}}{(\tilde{\alpha} + \tilde{\lambda})^2}\end{aligned}\quad (\text{C8})$$

### Ridgeless limit as exactly solvable model

The solution to the self-consistent equation for  $\tilde{\lambda}$  in the limit  $\lambda \rightarrow 0$  becomes

$$\tilde{\lambda} = \begin{cases} 1 - \tilde{\alpha}, & \tilde{\alpha} < 1 \\ 0, & \tilde{\alpha} \geq 1 \end{cases}, \quad (\text{C9})$$

and the self-consistent equation for  $\tilde{\varepsilon}$  simplifies to:

$$\tilde{\varepsilon} = \begin{cases} \frac{\tilde{\varepsilon}}{\sqrt{E_\infty}} \sqrt{1 - g(\tilde{\varepsilon})\tilde{\alpha}} \left( 1 + \frac{1 - E_\infty}{E_\infty} \frac{1}{\left( 1 + \frac{\tilde{\alpha}}{1 - \tilde{\alpha}} \frac{1 + \sigma^2\beta}{1 + \sigma^2(1 - \beta)} \right)^2} \right)^{-1/2}, & \tilde{\alpha} < 1 \\ \frac{\tilde{\varepsilon}}{\sqrt{E_\infty}} \sqrt{1 - g(\tilde{\varepsilon})\tilde{\alpha}^{-1}}, & \tilde{\alpha} \geq 1 \end{cases}. \quad (\text{C10})$$

Assuming non-zero  $E_\infty > 0$ , this reduces to the following transcendental equation at the capacity  $\tilde{\alpha} = 1$

$$\tilde{\varepsilon} = d' \sqrt{1 - g(\tilde{\varepsilon})}, \quad (\text{C11})$$

where we defined the discriminability  $d' \equiv \frac{\varepsilon}{\sqrt{E_\infty}}$ . We asymptotically extract its behavior for large and small  $d'$ . Note that the range of  $\tilde{\varepsilon}$  is  $[0, d']$ , since the function  $1 \geq g(x) > 0$ .

For large  $d' \gg 1$ ,  $\tilde{\varepsilon}$  gets large and approaches to  $d'$ . Expanding the function  $g$  in this limit as  $g(\tilde{\varepsilon}) \approx \frac{2}{\tilde{\varepsilon}^2}$ , we get

$$\tilde{\varepsilon} \approx d'(1 - d'^{-2}), \quad d' \gg 1. \quad (\text{C12})$$

Similarly, for small  $d' \ll 1$ , the argument approaches to zero and admits the expansion  $g(\tilde{\varepsilon}) \approx 1 - \sqrt{\frac{2}{\pi}} \tilde{\varepsilon}$ . Replacing this and squaring both sides, we obtain

$$\tilde{\varepsilon} \approx \sqrt{\frac{2}{\pi}} d'^2, \quad d' \ll 1. \quad (\text{C13})$$

In Fig. S1, we confirm the validity of this approximation against its numerical solution.

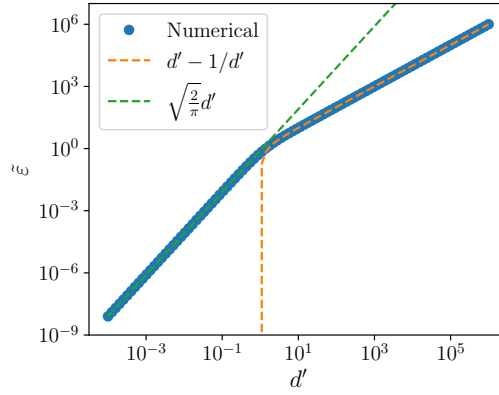


FIG. S1. Comparison of the numerical solution to Eq. C11 to its asymptotic behavior.

#### Appendix D: Spectral Decomposition

Previously, we had formulated our theory in terms of the covariance matrices of representations where we defined the functions

$$\begin{aligned} \mathcal{F}(\tilde{\lambda}, \tilde{\varepsilon}) &= \text{tr} \Sigma_\psi \mathbf{G}^{-1}, \quad \mathbf{G} = \mathbf{I} + \frac{\tilde{\alpha}}{\tilde{\lambda}} \Sigma_\psi, \quad \gamma = \partial_{\tilde{\lambda}} \mathcal{F}(\tilde{\lambda}, \tilde{\varepsilon}) \\ \mathcal{G}(\tilde{\lambda}, \tilde{\varepsilon}) &= \frac{E_\infty + \text{tr} \mathbf{w}_* \mathbf{w}_*^\top \Sigma_\psi \mathbf{G}^{-2}}{1 - g(\tilde{\varepsilon}) \gamma} \\ E_\infty &= \text{tr} \bar{\mathbf{w}} \bar{\mathbf{w}}^\top \Sigma_{\bar{\psi}} - \text{tr} \mathbf{w}_* \mathbf{w}_*^\top \Sigma_\psi, \quad \mathbf{w}_* = \Sigma_\psi^{-1} \Sigma_{\psi \bar{\psi}} \bar{\mathbf{w}} \end{aligned} \quad (\text{D1})$$

where  $\tilde{\lambda}$  and  $\tilde{\varepsilon}$  obey the coupled self-consistent equations given in Eq. 5. Here, we cast our formulas in terms of the spectral properties of representations. Following the kernel notation in [12, 14], the covariance matrices above are given by:

$$\begin{aligned} \Sigma_\psi &= \int \psi(\mathbf{x}) \psi(\mathbf{x})^\top d\mu(\mathbf{x}) \\ \Sigma_{\bar{\psi}} &= \int \bar{\psi}(\mathbf{x}) \bar{\psi}(\mathbf{x})^\top d\mu(\mathbf{x}) \\ \Sigma_{\psi \bar{\psi}} &= \int \psi(\mathbf{x}) \bar{\psi}(\mathbf{x})^\top d\mu(\mathbf{x}), \end{aligned} \quad (\text{D2})$$

where  $d\mu(\mathbf{x})$  is the distribution of the inputs and we treat representations  $\boldsymbol{\psi}(\mathbf{x})$  and  $\bar{\boldsymbol{\psi}}(\mathbf{x})$  as feature maps. We also express the target function and predictor as

$$\begin{aligned}\bar{y}(\mathbf{x}) &= \bar{\mathbf{w}} \cdot \bar{\boldsymbol{\psi}}(\mathbf{x}), \\ y(\mathbf{x}) &= \mathbf{w} \cdot \boldsymbol{\psi}(\mathbf{x}).\end{aligned}\tag{D3}$$

Note that the asymptotic error is simply the variance of the target function minus the variance of its projection to the learnable subspace:

$$E_\infty = \|\bar{y}(\mathbf{x})\|_2^2 - \|\bar{y}_\parallel(\mathbf{x})\|_2^2 = \|\bar{y}_\perp(\mathbf{x})\|_2^2,\tag{D4}$$

which is the unexplainable variance as  $\alpha \rightarrow \infty$ . Note that the explainable portion of the target function can also be obtained by (Eq. D1):

$$\bar{y}_\parallel(\mathbf{x}) = \mathbf{w}^* \cdot \boldsymbol{\psi}(\mathbf{x}) = \int d\mu(\mathbf{x}') \bar{y}(\mathbf{x}') \left( \boldsymbol{\psi}(\mathbf{x}')^\top \boldsymbol{\Sigma}_\psi^{-1} \boldsymbol{\psi}(\mathbf{x}) \right),\tag{D5}$$

where the term in the parenthesis can be considered as a projection kernel in the space of square-integrable functions. This allows us to diagonalize our formulas in the basis of  $\boldsymbol{\Sigma}_\psi$ .

We want to study generalization error in regards to task-model alignment and spectral bias [14] and hence need to obtain the decomposition of the target in the space of square-integrable functions expressible by the feature map  $\boldsymbol{\psi}(\mathbf{x})$  via regression. These functions belong to the function space associated with the inner-product kernel  $K(\mathbf{x}, \mathbf{x}') = \boldsymbol{\psi}(\mathbf{x})^\top \boldsymbol{\psi}(\mathbf{x}')$  and can be diagonalized as

$$K(\mathbf{x}, \mathbf{x}') = \boldsymbol{\psi}(\mathbf{x})^\top \boldsymbol{\psi}(\mathbf{x}') = \sum_i \lambda_i \phi_i(\mathbf{x}) \phi_i(\mathbf{x}'); \quad \int \phi_i(\mathbf{x}) \phi_j(\mathbf{x}) d\mu(\mathbf{x}) = \delta_{ij},\tag{D6}$$

where  $\{\lambda_i\}$  are non-negative eigenvalues of the kernel and  $\{\phi_i(\mathbf{x})\}$  is a set of complete eigenfunctions with respect to the measure  $d\mu(\mathbf{x})$ . While there are infinitely many eigenfunctions with respect to  $d\mu(\mathbf{x})$ , there at most  $\dim(\boldsymbol{\psi})$  non-zero eigenvalues. We define the index set  $\mathcal{I}^+ = \{i \mid \lambda_i > 0\}$  for positive eigenvalues and  $\mathcal{I}^0 = \{i \mid \lambda_i = 0\}$  for vanishing eigenvalues. On the other hand, target function generically may have infinitely many components

$$\bar{y}(\mathbf{x}) = \sum_i \bar{a}_i \phi_i(\mathbf{x}); \quad \bar{a}_i = \int \bar{y}(\mathbf{x}) \phi_i(\mathbf{x}) d\mu(\mathbf{x}),\tag{D7}$$

where  $\{\bar{a}_i\}$  are target coefficients.

Then the equations in Eq. D1 can be written as

$$\begin{aligned}\mathcal{F}(\tilde{\lambda}, \tilde{\varepsilon}) &= \frac{\tilde{\lambda}}{N} \sum_{i \in \mathcal{I}^+} \frac{\lambda_i}{\tilde{\lambda} + \tilde{\alpha} \lambda_i}, \quad \gamma = \frac{1}{N} \sum_{i \in \mathcal{I}^+} \frac{\tilde{\alpha} \lambda_i^2}{(\tilde{\lambda} + \tilde{\alpha} \lambda_i)^2} \\ \mathcal{G}(\tilde{\lambda}, \tilde{\varepsilon}) &= \frac{1}{1 - g(\tilde{\varepsilon})\gamma} \left( \sum_{i \in \mathcal{I}^0} \bar{a}_i^2 + \sum_{i \in \mathcal{I}^+} \frac{\tilde{\lambda}^2}{(\tilde{\lambda} + \tilde{\alpha} \lambda_i)^2} \bar{a}_i^2 \right),\end{aligned}\tag{D8}$$

which exactly matches the equations from [14] for  $\varepsilon = 0$  up to rescaling  $\lambda_i \rightarrow N\lambda_i$ .

This form enables us to analyze the generalization error from an error mode geometry perspective introduced in [32]. Error mode geometry relates linear predictivity to the geometric properties of representations based on the observation that the generalization error for ridge regression can be decomposed as a sum of mode errors associated with each spectral component [12, 14, 32]. Error modes are defined as

$$W_i(\tilde{\alpha}) \equiv \frac{\tilde{\lambda}^2}{1 - g(\tilde{\varepsilon})\gamma} \frac{\bar{a}_i^2}{(\tilde{\lambda} + \tilde{\alpha} \lambda_i)^2}, \quad E_g = \sum_i W_i(\tilde{\alpha})\tag{D9}$$

and corresponds to the unexplained variance in the  $i^{\text{th}}$  eigendirection. Note that with increasing  $\alpha$ , the contribution of each mode  $\bar{a}_i^2$  decreases with a rate proportional to the inverse eigenvalue  $\lambda_i^{-1}$  associated with that mode, revealing the fact that variances associated with small eigenvalues require more samples to be reduced. Error mode geometry refers to the summarization of these error modes in terms of radius and dimensionality defined as:

$$R_{em} = \sqrt{\sum_i W_i(\tilde{\alpha})^2}, \quad D_{em} = \frac{(\sum_i W_i(\tilde{\alpha}))^2}{\sum_i W_i(\tilde{\alpha})^2}\tag{D10}$$

which explicitly relates to the prediction error  $E_g = R_{em} \sqrt{D_{em}}$ .

## Appendix E: Experimental Details

Experimental details and the code reproducing the figures can be accessed from [https://github.com/canatar/svr\\_code](https://github.com/canatar/svr_code).

## Appendix F: Additional Experiments

### 1. Effect of Target-Noise Correlation

Even in the presence of noise in the representations, large correlations  $\beta$  between noise and the coding direction  $\bar{\mathbf{w}}$  cause more uncertainty in the predictions and, therefore, affect the precision. In Fig. 4, we show this effect for various  $\beta$ , where the noise geometry varies between completely orthogonal and parallel to the coding direction.

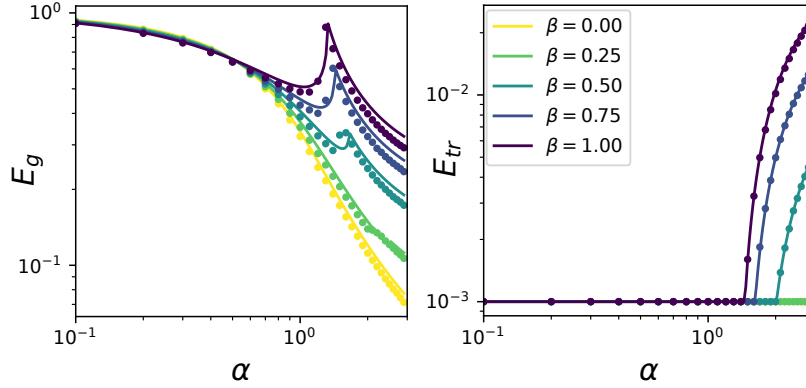


FIG. S2. Theoretical (lines) and experimental (dots) learning curves for the toy model with  $\sigma = 0.5$  and  $\epsilon = 0.5$ . With the same noise strength, increasing the alignment between the noise and coding direction affects the generalization adversely.

### 2. Error Mode Geometry of Real Data

Here, the metrics introduced in [32] and summarized in SI.D are applied to the experiment presented in Fig. 5. We show how the error mode geometry decomposition compares to the optimal tube size in Fig. S3. From input representation to the first layer, dimensionality  $D_{em}$  drives explain lower values of  $\epsilon_{opt}$  despite the increase in  $R_{em}$ . For random networks, dimensionality across the layer hierarchy decreases, while for the trained networks dimensionality remains the same except for the peak in the last layer. This can be related to the fact that later layers of trained networks are more task-tailored and, hence, become invariant to nuisance variations. Furthermore, we compare the

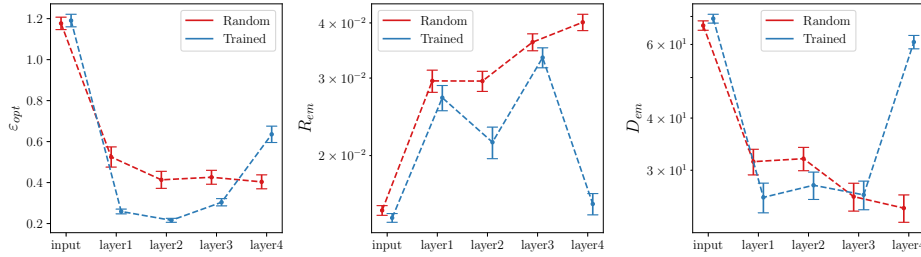


FIG. S3. Comparing optimal tube size to error mode geometry [32].

optimal tube size to the representational properties independent of  $\alpha$ . We define the participation ratios for the



eigenvalues and alignment coefficients as

$$\text{PR}(\lambda) = \frac{(\sum_i \lambda_i)^2}{\sum_i \lambda_i^2}, \quad \text{PR}(W) = \frac{(\sum_i W_i(0))^2}{\sum_i W_i(0)^2} = D_{em}(0) \quad (\text{F1})$$

which respectively characterize the dimensionality of the neural code and distribution of target components across the model's eigenbasis. In Fig. S4, we compare optimal tube size to these measures.

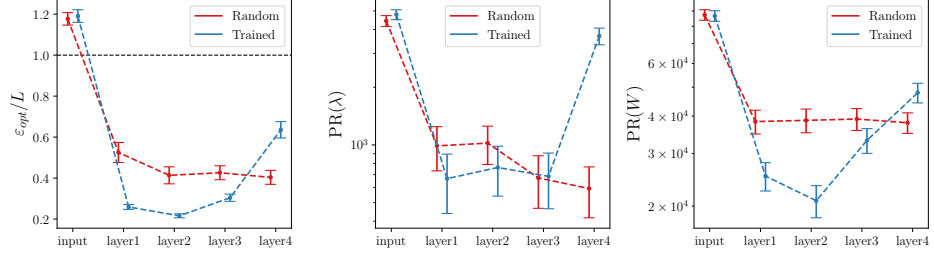


FIG. S4. Comparing the optimal tube size to participation ratios of eigenvalues and alignment coefficients.